Atoms in Optical Potentials: The Lèvy-Kicked Rotor

A thesis submitted towards partial fulfilment of
BS-MS Dual Degree Programme

by

Md. Noaman

under the guidance of

Dr. Umakant Rapol

Assistant Professor

Indian Institute of Science Education and Research
Pune

Certificate

This is to certify that this thesis entitled 'Atoms in Optical Potentials: The Lévy-Kicked Rotor' submitted towards the partial fulfilment of the BS-MS dual degree programme at the Indian Institute of Science Education and Research Pune represents original research carried out by Md. Noaman at 'Indian Institute of Science Education and Research, Pune', under the supervision of Dr. Umakant Rapol during the academic year 2012-2013.

Student
Md. Noaman

Supervisor
Dr. Umakant
Rapol

Acknowledgements

I thank my guide, Dr. Umakant Rapol for providing me the opportunity to work in his lab. I have found a great listener and a dexterous experimenter in him which was a continuous source of inspiration. In addition, his continuous encouragements were the most helpful whenever I needed.
I thank Dr. M S Santhanam for the discussions over the theoretical aspects of this project. His efforts, ultimately, made me realize the importance of this project.
I thank Anees Ahmed for the discussions over the various models in the many-body physics which helped me decide my future area of study. I thank Iti Kapoor for her help and conversations during the tough times. I thank Anirban Chowdhury for encouragement and bringing me smile even in a tense situation. I am thankful to Jammi Sindhu for the discussions over the project. I thank Sunil Kumar and Sumit Sarkar for making the lab environment entertaining. Their support and help with the experiment were fruitful for me. I thank Gunjan Verma for her asking me a lot of questions which ultimately cleared up few of my confusions also. I thank Tomin James and Chetan Vishwakarma for, again, their wonderful and sometimes crazy questions which helped me learn to explain things in a better way. My special thanks go to Prashant Kale and Neelesh Dumbre for their help and support in the lab.
I thank my family members Aman, Farhat and Irfan for their help and emotional supports during the entire period. It was a great source of enjoyment listening to the laughs of little Aleena. Lastly, but the most I am thankful to my parents who provided me all facilities and supports without that I wouldn't have been to this position.

Abstract

The invention of laser cooling and trapping techniques for neutral atoms provides a platform to visualize quantum effects associated with matter. In addition, this technique lends control and manipulation of the factors that reflect changes in the dynamics of a system in quantum regime. One of such examples is a kicked rotor system. Particles in a delta kicked spatially periodic potential, mimics this system. The dynamical evolution of this system in the quantum regime is very different from that in a classical regime. Average energy of a classical system increases linearly as the number of kicks increases whereas, for a quantum system, the average energy saturates to a certain limit. This key feature of saturation in a quantum system is caused by suppression of momentum diffusion. At this point, the system is analogous to a crystal with defects that shows localization of electrons near lattice sites, popularly known as Anderson localization. The energy-time relation of a kicked rotor system can be mapped to the position-momentum relation of such a defective crystal. This deviation in energy evolution can be considered as a 'meter-scale' to understand the transition from quantum to classical regime. Small amount of noise coupling to a quantum system leads to decoherence in the evolution of the system. For a classical system the energy gained by the system does not saturate, instead, it increases linearly with increase in number of kicks. By increasing the amount of noise, the system can undergo a complete transition to the classical regime. The noise could be generated by various means such as noise in amplitude of each kicks, fluctuation in the periodicity of the kicks or any other mechanism which causes loss in coherence. It has been predicted that noise in the periodicity of kicks, where the periodicity follows Lèvy's statistics the decoherence is suppressed. In fact, in certain parameter space, the decoherence-time increases to infinity. This is very important to prepare decoherence free system for experiments such as quantum information processing and quantum emulation. The use of ultra-cold atoms is very important because as the temperature goes down, the momentum distribution confines to very small range. The corresponding wavelength of the particles becomes large enough to observe the interference effect and therefore the atoms' energy reaches a state where quantum behaviour dominates. Red detuned counter propagating laser beams can be used to create periodic optical potentials. Fast flashes of such field, given on ultra-cold atoms exactly mimics a kicked rotor system. This system is very simple to study the dynamical evolution with the additional noise. We trap

Rb atoms in Magneto-optic Trap and further cool them down by Sysiphus cooling to prepare particles for the experiment. At temperature below 10 μK, flashes of standing wave are applied to the atoms which leads to re-distribution of momenta of the atoms. After certain time of free evolution, atoms are imaged to observe the momentum distribution and consequently the measurement of the energy. In this thesis, we report the progress towards experiments to study the evolution of system in which periodicity of the kicks follows Lèvy's statistics.

Contents

Chapter 1

Introduction

1.1 History

The idea of laser cooling and trapping of atoms is a relatively new development. The technique was first by T W Hänsch and Schawlow [1] for neutral atoms and by D. Wineland and H Dehmelt [2] for ions in 1975. They proposed a method to directly target each atom and slow them down to certain minimum limit which is set by the Doppler effect. In a pair of counter-propagating light when an atom moves it 'sees' different shift in the frequency of the light coming from the two directions. At a condition when the frequency of light is tuned slightly below the transition frequency of the atomic level, the atom 'sees' the light which is opposite to their velocity more close to resonance. And therefore, the atom absorbs photons more frequently from the light which is opposite to the direction it moves. As a result the net momentum is imparted to the atom is in the direction opposite to its velocity. Consequently, the excited-state atom comes to ground state by emitting a photon in random direction. Because, the emission of photon is in random direction, the net momentum-gain turns out to be zero. So, over many absorption-emission cycles the atoms get slowed down and the temperature, which is a measure of the spread in the momenta of a sample of particles, reduces. The first experimental observation was done by S. Chu et al [3] in 1985. Because atoms 'feel' the environment created by the light field as a 'viscous medium' like molasses, it is commonly known as 'optical molasses'. Though the atoms are cold in the light field but to perform any experiment they need to be confined in space. The spatially dependent force is created by additionally producing an inhomogeneous magnetic field. The field splits up the energy levels commonly known as Zeeman splitting of the atomic transition lines. By choosing appropriate polarization of the beams

the atoms feel a potential minimum towards a position where the magnetic field is zero. Creating an inhomogeneous field with such minimum is possible with a pair of coils in anti-helmholtz configuration. This was first observed by Raab et al [4] in 1987 and it is popularly known as Magneto-Optic Trap (MOT). The temperature of the atoms after this step is generally of order 100's of μK which is limited by the photons that are emitted randomly from the excited-state atoms. At such low temperature the average velocity of the atoms is of order few m/s which is low enough to observe certain quantum effects. It has become a routine task to create MOT as a basic platform for performing experiments in the areas of ultra-cold atoms. Though the temperature is very low, it is not sufficiently low enough to observe another state of matter which is defined for a quantum system with all particles in single state: the Bose-Einstein Condensate (BEC) [5, 6]. Since, the temperature is limited by the scattering of photon form a near resonant light; therefore ideas were implemented to use a pure magnetic field to trap atoms and then further cooled by throwing away the high energy atoms from the ensemble. This method of cooling is known as 'evaporative cooling' which is exactly analogous to the way a cup of coffee is cooled down. The difference here is that the hot atoms are thrown away with the help of radio frequency which flips the spin state of atoms such that they feel a repulsive potential in the magnetic trap. Simultaneously, increasing the confining strength, by increasing magnetic field gradient, atoms attain high phase-space density which is desirable condition for the BEC. First observation of BEC was made in 1995 by Eric Cornell and Carl Wieman at NIST [7] and W Ketterle at MIT [8].

1.2 Overview

The technical advancements in laser cooling and trapping of atoms have opened up a path to study various interesting physics [9], hitherto, which was very difficult with the already existing alternatives. For example, trapping atoms in optical lattice creates a situation which is a close resemblance of a real crystal [10]. This gives us freedom to tune many other parameters relevant to a crystal. Various models proposed in theory [11] are being tested. Additionally, achievement of atomic clocks for precision measurement of time and consequently frequency is one of such examples which has modified the definition of time [12, 13]. Few of the practical uses are accurate measurement of location using GPS devices, validation of the theoretical results in relativity and precision metrology [14].
The main interest in this thesis is towards understanding the transition of a system from quantum domain to classical domain. Theoretically, this can be

seen as setting the value of $\hbar$ to zero and all the result starts following as a classical system. But, this is not a correct way to proceed; though the value of $\hbar$ is small but still it is not zero for any case. In this thesis, the main focus is to experimentally realize the quantum classical correspondence principle and the factors that lead towards this transition. A delta kicked rotor system, which is actually a particle in a periodic potential with the potential turns on for a very short time repeatedly after certain fixed time interval, is taken as a model to probe this phenomenon. The dynamics of a delta kicked rotor in classical regime itself is very interesting as it shows, just by varying one parameter, a transition from predictable phase-space diagram to completely chaotic behavior. The behavior of this system in quantum regime is completely different from that in the classical domain [15]. In the classical domain where the momentum of the system becomes random and therefore the average energy follows a linear increment as time increases whereas in the quantum domain the evolution of energy doesn't follow this. The particles pick up only certain set of momenta which lead to saturation in the average energy. This distinction makes a delta kicked rotor tool to measure the transition from quantum to classical domain. This transition can be seen by adding noise into the system by various means such as letting some resonant light, adding noise in the periodicity or the amplitudes of the kicks [16, 17]. The simplicity of this system makes it experimentally very attractive. Ultra-cold atoms in an optical lattice which is flashed on for very short time repeatedly is the experimental realization of delta kicked rotor [18].
Additionally, if the periodicity of the kicks doesn't remain fixed but it follows certain statistics, in particular lèvy statistics [19], the dynamics in quantum regime is shown to lead to interesting results. In general, the de-coherence time follows an exponential decay, but in the case lèvy distributed periodicity, this doesn't remain valid and the de-coherence time increases to infinity in certain scenerio. Which shows that de-coherence is ill defined. The extended coherence length is very useful while performing experiments such as quantum computation and quantum emulation, because long lived states are one of the basic needs for these experiments.

1.3 Outline of the thesis

In this section a brief introduction to the following chapters are given. Chapter 2 covers the theoretical background needed for understanding the technique of laser cooling. This also contains the theoretical background of the physics related to quantum kicked rotor. Chapter 3 describes the details of experimental methods that are needed for laser cooling and trapping. In

addition, in this chapter we present the details of the experiments for creating optical lattices and producing the kicks. Chapter 4 contains the results obtained from the experiments. In Chapter 5 the ideas of performing experiments with the kicked rotor system has been discussed. Additionally, the future plans with the existing system is also mentioned.

Chapter 2

Theory

The realization of kicked rotor in the quantum domain requires certain conditions which are well satisfied by cold atoms. In this chapter, detailed theoretical frame-work is introduced which is necessary to understand the mechanism of laser cooling and consequently the physics of quantum delta kicked rotor. Additionally, the requirement of optical lattice is also discussed in this chapter.

2.1 Two-Level System

In this section we build the understanding of the interaction of a two-level atom coupled to light, under the assumption that an atom behaves as an electric dipole. This is a valid assumption as long as the multi-pole terms do not play big role which is acceptable when the light intensity is not very high (the corresponding electric field should be less than the field created by the nucleus). We use laser for the interactions because it shows various properties, for example it is monochromatic, coherence which make it simple to understand the interactions.

2.1.1 Atom-Light Interaction

Consider a two-level system which has a ground state g and an excited state e and the two states are coupled with an external light field. The atom interacts with a laser beam of frequency ω and therefore the detuning from the resonance will be $\Delta = \omega - \omega_0$, where ω_0 is atomic transition frequency. The following calculations are mostly followed from ref [20].
The evolution of the system is governed by the time dependent Schrödinger

equation.

$$i\hbar\frac{\partial\psi(\mathbf{r},t)}{\partial t} = H\psi(\mathbf{r},t) \tag{2.1}$$

The atomic wave function can be expressed in the linear superposition of ground and the excited state as:

$$\psi(\mathbf{r},t) = c_g(t)|g\rangle + c_e(t)|e\rangle \tag{2.2}$$

And the Hamiltonian, $H = H_0 + V$, where H_0 is the Hamiltonian of the unperturbed atom with the eigenstates $|e\rangle$ and $|g\rangle$, and $V = \mathbf{d}\cdot\mathbf{E}$ where $\mathbf{d}$ is dipole moment and $\mathbf{E}$ is electric field associated with the light field.
Inserting Eq. (2.2) into Eq.(2.1) we get two coupled equations corresponding to two levels:

$$i\hbar\frac{dc_g(t)}{dt} = c_e\langle g|bfd\cdot\mathbf{E}|e\rangle e^{-i\omega_0 t} \tag{2.3}$$

$$i\hbar\frac{dc_e(t)}{dt} = c_g\langle e|\mathbf{d}\cdot\mathbf{E}|g\rangle e^{+i\omega_0 t} \tag{2.4}$$

For a plane wave, the electric field can be written as $\mathbf{E} = bf\epsilon\mathbf{E}_0 cos(\mathbf{k}\cdot\mathbf{r}-\omega t)$. Using this in equations (2.3) and Eq. (2.4) we get us the following set of equations:

$$i\hbar\frac{dc_g(t)}{dt} = c_e\hbar\Omega^*(\frac{e^{i(\omega-\omega_0)t}+e^{-i(\omega+\omega_0)t}}{2}) \tag{2.5}$$

$$i\hbar\frac{dc_e(t)}{dt} = c_g\hbar\Omega(\frac{e^{i(\omega+\omega_0)t}+e^{-i(\omega-\omega_0)t}}{2}) \tag{2.6}$$

where Ω is the *Rabi Frequency*[20] and describes the strength of coupling between the two levels and the field intensity.

$$\Omega = \frac{\mathbf{E}_0}{\hbar}\langle e|\mathbf{d}\cdot\epsilon|g\rangle \tag{2.7}$$

Now, to make this problem simpler, we make an assumption which is based on averaging out the fast oscillating term in the two coupled equations. This assumption is known as *Rotating Wave Approximation* (RWA) which assumes that the term $e^{-i(\omega+\omega_0)}$ oscillates very fast when the frequency difference is not very large and therefore this term can be eliminated as the time dependence averages out over much slower timescale of the evolution of the coefficients c_g and c_e.
The equations (2.5) and (2.6) can further be simplified to:

$$i\hbar\frac{dc_g(t)}{dt} = c_e\hbar\Omega^*\frac{e^{i\Delta t}}{2} \tag{2.8}$$

$$i\hbar\frac{dc_e(t)}{dt} = c_g\hbar\Omega\frac{e^{-i\Delta t}}{2} \tag{2.9}$$

In order to remove the explicit time dependence on the right hand side of the two equations, (2.8) and (2.9) can be reformulated by introducing new set of coefficients $c'_g = c_g$ and $c'_e = c_e e^{i\Delta t}$.

$$i\hbar\frac{dc'_g}{dt} = c'_e\frac{\hbar\Omega}{2} \tag{2.10}$$

$$i\hbar\frac{dc'_e}{dt} = c'_g\frac{\hbar\Omega}{2} - c'_e\hbar\Delta \tag{2.11}$$

the Hamiltonian can, now be written as:

$$H = \frac{\hbar}{2}\begin{bmatrix} 0 & \Omega \\ \Omega & -2\Delta \end{bmatrix} \tag{2.12}$$

By diagonalizing the matrix, we easily find the eigenvalues, $E_g = \frac{\hbar}{2}(-\Delta - \sqrt{\Omega^2 + \Delta^2})$ and $E_g = \frac{\hbar}{2}(-\Delta + \sqrt{\Omega^2 + \Delta^2})$. The shift in the energy eigenvalues of the two levels caused by presence of light is called *light shift* or the *AC Stark Shift*. For a far detuned light the square root term can be expanded and the energy shift $\Delta E = \frac{\hbar\Omega^2}{4\Delta}$ which is proportional to the light intensity. The shift in the energy of the ground state and the excited state is opposite to each other. The eigenstates get modified as:

$$|e'\rangle = cos\theta|g\rangle - sin\theta|e\rangle; \quad |g'\rangle = sin\theta|g\rangle + cos\theta|e\rangle \tag{2.13}$$

where $cos\theta = -\Delta/\Omega'$. These states are known as dressed states as the bare atoms are 'dressed' by the presence of off-resonant light field. Each state can be represented as a coherent superposition of the two bare atomic states
Thus far we have been considering light as a classical entity and atom as a quantum system. To completely understand the interaction we must incorporate the interaction with the environment to atom. An illustration is given for this reason; since the atoms oscillate between the two states only in presence of light, therefore, the energy conservation suggests that either the atom absorbs a photon or it emits a photon of same frequency. And consequently, if the atom is prepared in excited state, it should never decay back to the ground state. But in real situation, atoms do not remain in a given state forever. And the reason is spontaneous emission, which is a result of atom interacting with environment. To understand these phenomena we use the density matrix method to study the dynamics.
The density operator of a given pure state is

$$\rho = |\psi\rangle\langle\psi| \tag{2.14}$$

The time evolution of density operator can be used to describe processes which are not handled with Hamiltonian equation such as spontaneous emission. Following is the equation of the time evolution density operator:

$$\frac{d\rho}{dt} = \frac{i}{\hbar}[\rho, H] \tag{2.15}$$

where the square brackets is the commutator of the density operator and the Hamiltonian. This is *Liouville's equation*, and it is equivalent to Schrödinger equation. The density matrix method also allows us to handle mixed states, in that case the density operator becomes:

$$\rho = \sum_i w_i |\psi_i\rangle\langle\psi_i| \tag{2.16}$$

A spontaneous emission process, which causes loss in the density of excited state that follows a decay rate Γ. The time evolution of the population is:

$$\frac{d\rho_{ee}}{dt} = -\frac{d\rho_{gg}}{dt} = -\Gamma\rho_{ee} \tag{2.17}$$

A similar effect of spontaneous emission on the off-diagonal term of the density matrix can be seen, as a result the time evolution is:

$$\frac{d\rho_{eg}}{dt} = -\Gamma\rho_{eg} \quad , \quad \frac{d\rho_{ge}}{dt} = -\Gamma\rho_{ge} \tag{2.18}$$

The full equation of motion for the density matrix, including the Hamiltonian part due to the interaction with external field and the spontaneous emission can be written as:

$$\frac{d\rho_{gg}}{dt} = \frac{i}{\hbar}[\rho, H] - \begin{pmatrix} -\Gamma\rho_{ee} & \frac{\Gamma}{2}\rho_{ge} \\ \frac{\Gamma}{2}\rho_{eg} & \Gamma\rho_{ee} \end{pmatrix} \tag{2.19}$$

using the commutator of ρ and H in Eq. (2.19) we get following equation for each of the matrix elements:

$$\dot{\rho}_{gg} = \frac{i\Omega}{2}(\rho_{ge} - \rho_{eg}) + \Gamma\rho_{ee} \tag{2.20}$$

$$\dot{\rho}_{ee} = -\frac{i\Omega}{2}(\rho_{ge} - \rho_{eg}) - \Gamma\rho_{ee} \tag{2.21}$$

$$\dot{\rho}_{ge} = -\frac{i\Omega}{2}(\rho_{ee} - \rho_{gg}) - i\Delta\rho_{ge} - \frac{\Gamma}{2}\rho_{ge} \tag{2.22}$$

$$\dot{\rho}_{eg} = \frac{i\Omega}{2}(\rho_{ee} - \rho_{gg}) + i\Delta\rho_{eg} - \frac{\Gamma}{2}\rho_{eg} \tag{2.23}$$

These are known as the *optical Bloch equations*. Out of these four equations we have two constraints; the sum of population $\rho_{ee} + \rho_{gg} = 1$ and the off-diagonal matrix elements are complex conjugates i.e. $\rho_{eg} = \rho^*_{ge}$. Only the three components $\{u, v, w\}$ of a vector known as *Bloch vector* which are important, are defined as follows:

$$u = \frac{1}{2}(\rho_{ge} + \rho_{eg}), \qquad v = \frac{1}{2\iota}(\rho_{eg} - \rho_{ge}), \qquad w = \frac{1}{2}(\rho_{gg} - \rho_{ee}) \tag{2.24}$$

The physical significance of the three terms are: w is proportional to the difference in the populations of the ground and the excited state, and u and v are respectively proportional to the in phase and quadrature components of the atomic dipole moment. The Bloch vector has maximum of unit length, and in the absence of spontaneous emission this unit vector defines a point on the *Bloch sphere*. The effect of spontaneous emission is to collapse the Bloch sphere; The Bloch vector no longer has unit length and the sphere eventually shrinks to a single point as all the atoms end up in the ground state.
We are interested in knowing the steady state solutions for constant Ω which can be obtained by setting the time derivative term to be zero. Thus we obtain

$$u_{ss} = \frac{\Delta}{\Omega}\frac{S}{1+S}, \quad v_{ss} = \frac{\Gamma}{2\Omega}\frac{S}{1+S}, \quad w_{ss} = \frac{1}{2}(\frac{S}{1+S} - 1) \tag{2.25}$$

where S is defined as saturation parameter given by:

$$S = \frac{\Omega^2/2}{\Delta^2 + (\Gamma^2/4)} = \frac{s}{1 + 4\Delta^2/\Gamma^2} \tag{2.26}$$

where the on-resonant saturation parameter $s = I/I_{sat}$. The I_{sat} is commonly used to describe the strength of transition as it is conveniently related to quantities that can be directly measured.
The dipole expectation $\langle \mathbf{d} \rangle$ can be expressed using the steady state solutions of the optical Bloch equation. In a density matrix formalism,

$$\langle \mathbf{d} \rangle = Tr(\rho d) = d_{eg}(\rho_{eg} + \rho_{ge}) \tag{2.27}$$

using $d_{ee} = d_{gg} = 0$ and $d_{eg} = d_{ge}$.
The expression for average force is defined as $\langle \mathbf{F} \rangle = \langle \mathbf{d} \cdot \mathbf{E} \rangle$ which under the assumption that the induced dipole is in the same direction as the electric field gives that $\langle \mathbf{F} \rangle = \langle \mathbf{d} \rangle \nabla \mathbf{E}$. Using equation(2.27) with the equations(2.25) in the force expression, we get the expression for the force by light on a two-level atom:

$$\mathbf{F} = -\frac{\hbar}{2}\frac{S}{1+S}(\frac{\Delta}{\Omega^2}\nabla\Omega^2 - \Gamma\nabla\theta) \tag{2.28}$$

2.1.2 Optical Forces on Atom

The equation (2.28) is general form of force that an atom feels when introduced to light field. The two terms in the force expression corresponds to two different regime. The one which is proportional to the gradient of intensity can be obtained from classical dipole force on an atom:

$$\mathbf{F}_{dip} = -\frac{\hbar}{2}\frac{S}{1+S}\frac{\Delta}{\Omega^2}\nabla\Omega^2 \tag{2.29}$$

This force is parallel to the direction of the intensity gradient and the sign of force is decided by the sign of detuning. For red detuned light the force is attractive towards the high-intensity regions and it is repulsive for blue detuned light towards the high-intensity regions. This important phenomenon leads to the principle of trapping atoms in a red detuned focused beam so called dipole trap.
The second term in the generalized force equation (2.28) describes the radiation pressure or the scattering force on the the atom, which is given by:

$$\mathbf{F}_{scatt} = \frac{\hbar\Gamma}{2}\frac{S}{1+S}\nabla\theta \tag{2.30}$$

This force is due to the spontaneous emission of photon from the excited atom and it is random by nature. The expression is ensemble average of many emission cycles. For a beam in single direction $\theta = \mathbf{k}\cdot\mathbf{R}$, which leads to $\nabla\theta = \mathbf{k}$ which means the force is in the direction of the propagation of light. The scattering forces do not preserve the phase relation of the atoms and therefore this leads to loss in coherence of a given quantum state.

2.1.3 Far Detuning Limit

The scattering forces are generally not favorable because they lead to dissipative effects which ultimately lead to loss of coherence. But, when the detuning of laser beam is varied and set farther apart from the atomic transition line, the saturation parameter, S up to some approximation gets modified to:

$$S = \frac{\Omega^2}{2\Delta^2} \tag{2.31}$$

where the detuning is set to large value ($\Delta^2 >> \Omega^2 >> \Gamma^2$).
The two forces:

$$\mathbf{F}_{scatt} = \frac{\hbar\Gamma\Omega^2}{4\Delta^2}\nabla\theta \tag{2.32}$$

$$\mathbf{F}_{dip} = -\frac{\hbar}{\Delta} 4\nabla\Omega^2 \tag{2.33}$$

Equations (2.32) and (2.33) shows interesting results while manipulating atom in light field. In addition to playing with the intensity of light, detuning also plays crucial role to control the effect of the scattering rate. By choosing far detuned light, the scattering rate which follows as $1/\Delta^2$, can be set to very small. On other hand the dipolar force follows as$1/\Delta$ which does not fall as rapidly as compared to the scattering force, this difference gives us control over manipulating the amount of dissipation in the system.

2.2 Laser Cooling

After having an understanding of the different kind of forces and their working regime, a direct application can be seen in the technique called laser cooling. The principle of this technique is based on the definition of temperature; particles at a given temperature occupy certain distribution of momentum. The spread in the momentum is a measure of temperature; larger width of the distribution corresponds to higher temperature of the system. Specially prepared laser beams can be used to target atoms based on their velocity such that the force becomes proportional to the velocity and in the opposite direction. This leads to slow the atoms down to a velocity distribution with narrow width and hence the reduction in temperature.

2.2.1 Optical Molasses

A pair of counter-propagating laser beams which are red detuned to the transition line of two-level atoms. The group of atoms which are moving faster see the light coming from the opposite direction more close to the resonance. As a result, these atoms scatter more photon from the beam which is opposite to the direction the atoms as compared to the other beam of light. This imbalance in scattering rate leads to a net force in the direction opposite to their velocity.
For near-resonance laser beam, the scattering force dominates. Expressing the force in terms of light intensity and detuning:

$$\mathbf{F}_{scatt} = \frac{\hbar\mathbf{k}\Gamma}{2} \frac{I/I_0}{1 + I/I_0 + [2\Delta/\Gamma]^2} \tag{2.34}$$

Since, the atoms are moving in the light field, they will feel the frequency of the light slightly shifted whose sign will be decided by the direction they

move. The shift is frequency $\delta = -\mathbf{k} \cdot \mathbf{v}$, will add up in the laser detuning term and modify the scattering rate. The modified force will be:

$$\mathbf{F}_{scatt} = \frac{\hbar \mathbf{k} \Gamma}{2} \frac{I/I_0}{1 + I/I_0 + [2(\Delta + \delta)/\Gamma]^2} \tag{2.35}$$

In the situation when two counter-propagating laser beams are shone to the atoms, the net force will be the sum of the two forces, $\mathbf{F}_{tot} = \mathbf{F}_+ + \mathbf{F}_-$, where

$$\mathbf{F}_\pm = \pm \frac{\hbar \mathbf{k} \Gamma}{2} \frac{I/I_0}{1 + I/I_0 + [2(\Delta \mp \delta)/\Gamma]^2} \tag{2.36}$$

adding the both terms, we get relation for the net force on the atom:

$$\mathbf{F}_{tot} \cong 8\hbar k^2 \Delta \frac{I/I_0}{\Gamma(1 + I/I_0 + (2\Delta/\Gamma)^2)^2} \mathbf{v} = -\beta \mathbf{v} \tag{2.37}$$

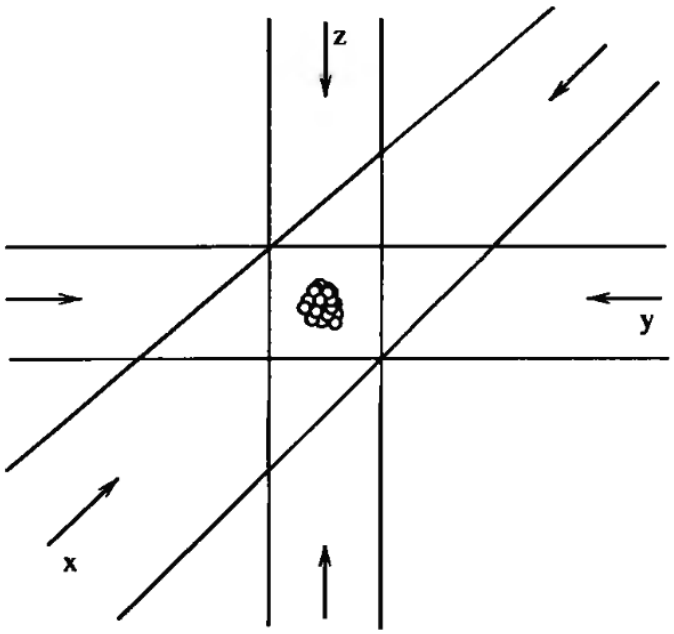

Figure 2.1: 3-Dimensional setup for optical molasses [20]. Red detuned counter-propagating laser beams are shone from the three orthogonal directions. The overlap region creates the 'optical molasses'

The force is proportional to velocity but in opposite direction, therefore it opposes the movement of the atoms. This 'viscous' medium is known as *optical molasses*. In an arrangement (see fig. 2.1), where three pairs of

counter-propagating laser beams are shone, the cross-over region creates a region which opposes the velocity of an atom from all the three orthogonal directions. Atoms within the trap-depth of the potential created by the laser field gets slowed down and therefore the temperature of these atoms reduces down to certain minimum value which is limited by so called *Doppler limit* [20].

2.2.2 Magneto-Optic Trap

The above mentioned technique is good enough to cool the atoms down to few 100's of μK, but the problem in this technique is that the atoms only get cooled down, there is no confinement where these cold atoms can be trapped for further experiments. There is no space dependent potential in this arrangement of light within the cross-over of the beams.
To create potential which is attractive at certain position, an inhomogeneous magnetic field created by a pair of coils in anti-Helmholtz configuration, is applied in addition to the optics arrangement. This creates quadrupole magnetic field which has minimum in the geometric center of the coils. Certain modification in the polarization of light is made in order to match with the condition required for trapping atoms in the center. Instead of using linearly polarized light now circular polarized light is used. This modification is made to satisfy the transition rules. In the presence of magnetic field, the magnetic sub-levels of atom get split. Figure 2.2 describes the 1-dimensional model of MOT where the energy levels get shifted by the additional magnetic field, which are position dependent. The shift in the magnetic sub-levels in magnetic field is $\mu' \cdot \mathbf{B}$, where $\mu' = (g_e M_e - g_g M_g)\mu_B$ is effective dipole moment for the transition. In the presence of σ^- light, the only possible transition occurs which satisfies $\Delta M = -1$ and therefore atoms at $z = z'$ are more close to resonance with the σ^- light as compared to the σ^+ light. This leads to enhanced scattering from the σ^- light and consequently the atom gets a biased push towards the center. If the atoms are in the left side of the field zero, more of σ^+ light starts scattering which again pushes the atoms to the center. A three dimensional schematic diagram is shown in the figure 2.3

The force by a pair of beams in the presence of magnetic field gets modified. The denuning term in the Eq. (2.36) now gets modified with the addition of the Zeeman shift. The modified detuning term δ is

$$\delta = \mathbf{k} \cdot \mathbf{v} - \mu' \cdot \mathbf{B}/\hbar \tag{2.38}$$

And therefore the net force is of the form:

$$\mathbf{F} = -\beta \mathbf{v} - \kappa \mathbf{r} \tag{2.39}$$

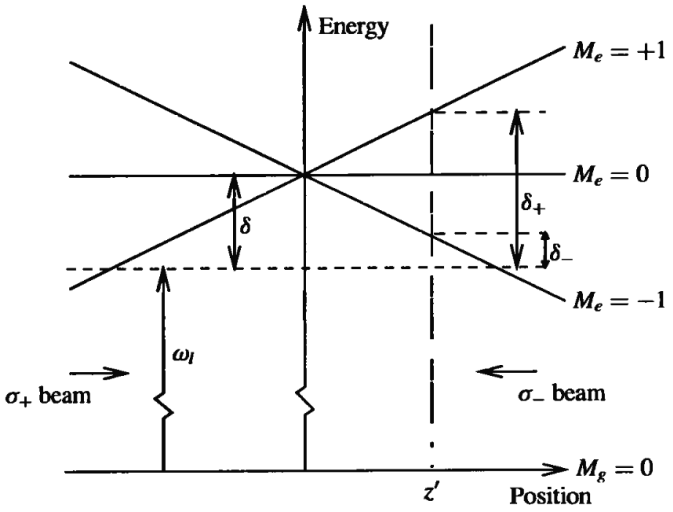

Figure 2.2: 1-dimensional setup for MOT [20]. Horizontal dashed line represents the laser frequency seen by atoms at rest in the center of the trap. Because of the Zeeman shifts of the atomic levels in the inhomogeneous magnetic field, atoms at $z = z'$ are closer to resonance with the σ^- laser beam than with the σ^+ beam, and are therefore forced towards the center of the trap.

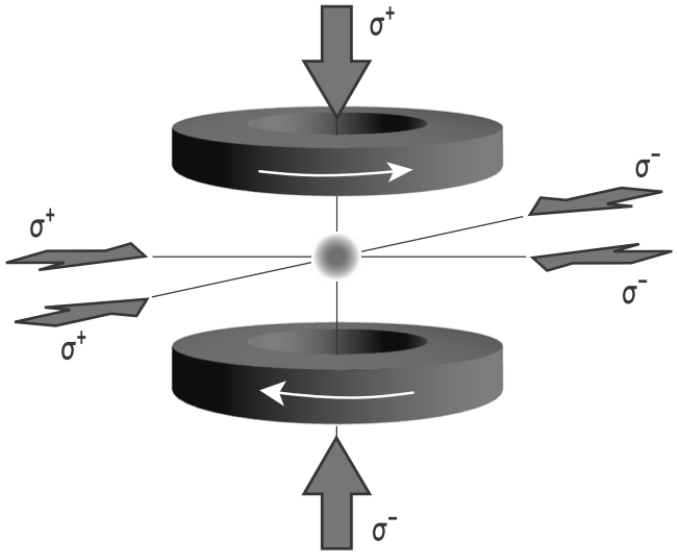

Figure 2.3: 3D schematic diagram of MOT [20]

where, the damping term β is defined in Eq. 2.37. The other term which is essentially a spring force makes the system confined near the center. The overall effect of both the light and the inhomogeneous magnetic field is to create a damped harmonic oscillator. The 'spring constant' κ arises from the force which is dependent on the Doppler shift and the Zeeman shift.

$$\kappa = \frac{\mu' \nabla \mathbf{B}}{\hbar k} \beta \tag{2.40}$$

MOT is one of the most important stages to start with in the area of experiments with ultra-cold atoms. This provides large number of cold atoms with temperature very low ($\sim$ 100's μK). The loading is not very sensitive towards slight imbalance in the laser power in the six beams or little mismatch in the alignment. The process of cooling in this section relies on the atomic velocity only by means of Doppler shift, and therefore it is commonly known as *Doppler cooling*. The temperature is limited by the line-width of the excited state and the atoms below certain velocity do not respond to any further cooling.

Zeeman Slower

To enhance the rate of loading of atoms in MOT the atoms need to slow down to the speed below the corresponding trap depth of the MOT. In many cases, atoms are released from an oven, and since they are at high temperature, the average velocity is very high ($\sim$ 300–400 m/s). Collimated high-velocity flux of atoms coming from the oven need to slow down to velocity about 25 m/s for fast loading. This can be done by, again, using the same principle of force applied by light on atoms. A beam of light opposite to the direction of the atomic beam is shone which opposes the motion of atoms leads to reduction in speed. Since the atoms are moving at high speed, the laser frequency needs to be detuned far enough to be scattered sufficiently large such that it forces the atoms significantly. But, just shifting the detuning will not be enough to make the atomic beam slow down to the required speed. The reason is once the atoms get slowed down, they no longer remain close to resonance and therefore the further scattering rate is reduced drastically and because of this the atoms do not get opposing force. To keep the atoms continuously under force, they need to be kept on resonance. This can be done, among the various other methods, by additionally applying a spatially varying magnetic field such that the Zeeman shift compensates for the detuning of the laser frequency and the detuning caused by the Doppler shift. As, it can be seen from the equation (2.34), only the detuning term gets modified in a similar fashion as with the MOT. Assuming, constant deceleration of atoms throughout the length, the maximum acceleration can be calculated and using the

force formula from the Eq. (2.34) other parameters such as laser detuning, laser power can be calculated.

2.2.3 Sisyphus Cooling

In this section the idea is to use the non-adiabatic mechanism to slow down the velocity of the atoms. This process is implemented with the use of optical pumping process and different light shifts for different magnetic sub-levels. In a configuration of two counter-propagating orthogonal linearly polarized light which creates spatially varying polarization of light from left circular to linear to right circular. Effectively there is a gradient of polarization. When the atoms are in a region where the polarization is σ_+, the atoms get excited with satisfying the condition $\Delta M = +1$ and subsequently they decay back to either of the sub-levels of the ground state. This process gives rise to a biased increase in population towards $\Delta M = +1$ state. Atoms, after certain number of absorption-emission cycles, end up in the positive magnetic sub-level of the ground state. Similarly, atoms in the σ_- region get pumped into the negative magnetic sub-levels of the ground state.
The change in polarization affects the light shifts of the atom. In low intensity condition, the ground state light shift is given by:

$$\Delta E_g = \frac{\hbar\Delta(I/I_0)C_{ge}^2}{1 + (2\Delta/\Gamma)^2} \tag{2.41}$$

where, C_{ge} is the Clebsch-Gordan coefficient which describes the coupling between the atom and the light field. The coefficient C_{ge} is dependent on the magnetic sub-levels which give rise to the different light shifts for different levels as shown in the fig. 2.4.

Consider an example of atoms with three ground-state sublevels. When an atom is at a position where the light is σ^+ polarized, after many absorption emission cycle it finally ends up in the $M_g = +1/2$ state. When it moves to $\lambda/4$ where the polarization is switched to σ^- the major population of the atoms is in the $M_g = -1/2$ sublevel. For, $\Delta < 1$ the light shift is negative and as the atom moves towards $\lambda/4$ it climbs up a potential barrier. This costs the reduction of kinetic energy of the atom. Once the atom is at the hill, by a mechanism of optical pumping it gets pumped to the lower light shifted state. The gained potential energy is carried away with the emitted photon. After certain number of such cycles, the atom gets slowed down to much lower velocity. The continuous climbing up a potential barrier is called *Sisyphus cooling*, the name inspired by Greek mythology. A three dimensional arrangement of such counter-propagating light beams makes the

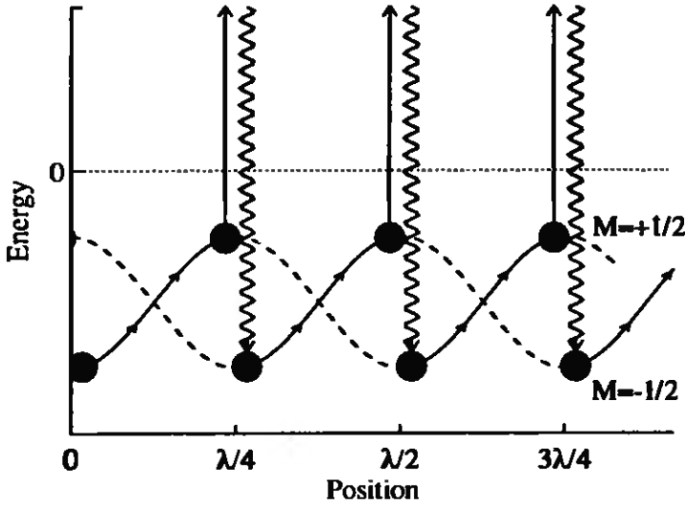

Figure 2.4: The spatial dependence of the light shifts of the ground-state sublevels [20]. As an atom with $M_g = +1/2$ sublevel at postion 0 moves towards $\lambda/4$ it feels a potential climb which slows then down. When the atom is at $\lambda/4$ it eventually gets pumped down to the $M_g = -1/2$ sublevel. The difference in energy is carried away by the emitted photon.

atomic cloud slow from all the directions.
In the practical experiment, we do not use the configuration of linearly perpendicular laser beams. It is also because the beams that are used for MOT are circularly polarized. In the case of two counter propagating orthogonal circular polarized light beams, the resultant field is linearly polarized with varying plane of polarization in the position space. As, shown by Dalibard and Cohen-Tannoudji [21], this case also works for sub-Doppler cooling.
Consider atoms with three magnetic sublevels. At a given position, atoms are distributed into the three sublevels, $M_g = 0, \pm 1$. Any change in the distribution is again refilled by the pumping mechanism due to the linearly polarized light which is nothing but combination of the two circular polarized light beams. This situation remains satisfied as long as the atoms are at rest in the light field. But, when the atoms move in some direction, the local polarization axis changes and subsequently the distribution of magnetic sublevels also changes. Therefore, the continuous pumping mechanism keeps on trying to repopulate to a distribution which was in a steady state condition. So, depending upon which side the atoms move, either the population in $M_g = +1$ sublevel or in $M_g = -1$ sublevel lags. It was shown in ref. [21], that when the atoms move towards σ^+ beam they populate more in the $M_g = +1$ sublevel than the $M_g = -1$ sublevel. Because of the different Clebsch-Gordan

coefficients for these two sublevels, atoms in $M_g = +1$ state scatters more σ^+ light than the σ^- light. Subsequently, these atoms after re-emission comes back to the same $M_g = +1$ sublevel. This imparts a continuous net force from $M_g = +1$ beam direction. Similar effect happens to the atoms which moves towards the σ^- beam. Three pairs of such beams can be arranged to suppress the velocity of the atoms from all the directions as a result the temperature goes down. The temperature in this step reduces down to few 10th of the temperature in the MOT which is very helpful for performing various experiments or transferring to the magnetic trap for further cooling.

2.3 Magnetic Trapping

Though, trapping atoms with optical forces in MOT and further cooled by polarization gradient cooling gives atoms at very low temperature, but it is still not sufficient to reach to certain interesting physical phenomena, like the Bose-Einstein Condensate (BEC). In these traps, the temperature is limited by the recoil energy transferred by the photon. Also, for obtaining denser cloud, the atoms need to be compressed in smaller region, which increases the light intensity and subsequently the scattering rate. And therefore, the temperature starts increasing. The idea further extends to trap neutral atoms in a potential which relies on the force exerted by the magnetic field. Atoms with magnetic dipole in the ground state or meta-stable states are good candidate for trapping in magnetic field created by a quadrupole coil.
Potential of an atom in a given magnetic field is:

$$V = g_F M_F \mu_B |\mathbf{B}| \tag{2.42}$$

where, $g_F M_F \mu_B$ is the magnetic dipole of an atom. g_F is lande g-factor, M_F is magnetic sublevel and μ_B is Bohr magneton.

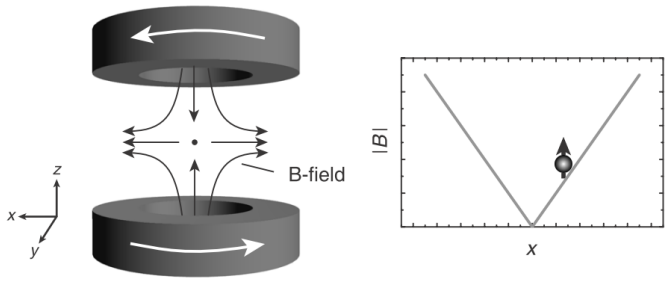

Figure 2.5: Schematic diagram of magnetic trap[20]

As it can be seen in Fig. 2.5, with a pair of coils in anti-Helmholtz configuration the magnetic field has minimum magnitude in the center. To create a trapping potential, the magnetic dipole moment should be chosen such that the atoms should 'feel' minimum energy in the center. This is possible only for positive magnetic dipole moment. For Rb-87 ground state $\mathbf{F} = 2$, $g_F = 1/2$ is a positive quantity (see fig. 3.2). Therefore atoms should be pumped to $M_F = +2$ state. Hence, before transferring atoms to the magnetic trap they need to be pumped into the positive magnetic sublevels. This is done by so-called optical pumping, where in presence of weak homogeneous magnetic field light of σ^+ polarization is shone to the atoms. σ^+ light excites the atoms to certain excited level with the condition that $\Delta M = +1$. When the atoms decay back, they occupy any of the possible magnetic sublevels of the ground state. Due to continuous cycling, the atoms finally end up populating the most positive sublevel.

2.4 Evaporative Cooling

We have seen that in the magnetic trap, for positive Lande g-factor, only atoms with positive magnetic sublevel get trapped. These sublevels are called low field seeking state. Similarly, the negative magnetic sublevel atoms move towards the higher field and are called high field seeking state. Therefore when the atoms are transferred, by some means, to the negative sublevel, they get out of the trap. The energy required to flip the state of a trapped atoms is $\Delta E = \mu_B |\mathbf{B}|(M_{(-F)}g_{(-F)} - M_{(F)}g_{(F)})$. The order of frequency for the energy needed to flip the state is 10's of MHz. Atoms in the magnetic trap is distributed as a thermal cloud. The particles with larger kinetic energy spend certain amount of time farther away from the trap center as compared to the slower atoms. Radio frequency which matches the transition frequency at a position farther away from the trap center is applied to flip the sublevel of the atoms which fall in that region. This flips the atomic magnetic state to un-trapped state and subsequently the atoms get out of the remainder of the cloud. Since the atoms which leave the trap are of higher kinetic energy, after thermalization the temperature of the remaining cloud reduces. By reducing the radio frequency, atoms with bit lesser kinetic energy also gets removed which makes the cloud even colder.

2.5 Optical Lattice

A pair of counter propagating linearly polarized light creates standing wave. Atoms, in such field feel a periodic potential because the intensity of light is periodic in space. This is equivalent to a crystal where electrons encounter similar potential as they move inside the crystal [10]. The potential of focused light in a retro reflecting manner is described by the following equation:

$$V(r,z) = -V_{lat}e^{-2r^2/w_0^2}sin^2(kz) \tag{2.43}$$

The intensity distribution is gaussian in the radial direction and it is periodic with periodicity, $k = 2\pi/\lambda$, v_{lat} is potential depth of optical lattice which can be obtained from the equation for dipolar force Eq. (2.33).
By crossing over two or three such standing wave, 2 dimensional or 3 dimensional periodic potential can be created. These give a tunable analog of crystal. In addition, this creates a pure form of the crystal with a tunable effective interaction. By changing angle of the standing wave pairs, different geometries can be realized. Laser frequency can also be tuned to change the lattice spacing. Various physics related to many-body system are being studied by the cold atoms in optical lattices [10].

2.6 Delta Kicked Rotor

If the potential is periodically flashed on and off, the such a potential is called a kicking potential as opposed to continuously driven potentials. Interesting features start showing up when the potential is spatially periodic which is sinusoidal in nature. A particle which feels such 'kicks' in a sinusoidally varying potential is called the kicked rotor [15]. The potential during the pulse on-time can be considered as perturbation, and since, the pulse width is very small, it helps reduce various complications involved while solving problems with time dependent perturbation. The system is very simple as there is nothing very complex interaction, like many body interaction, but, it shows very interesting results depending on the strength of the kicks [15]. The results are very different when the system is in quantum domain than when it is in classical domain. In the following subsections, we will see the dynamics of kicked rotor in different regimes. Since the classical and quantum behavior of the kicked rotor system is dramatically different, this system can be used to understand the effects of quantum to classical decoherence phenomena.

2.6.1 Classical Delta Kicked Rotor

A macroscopic system, whose dynamics is fully described by classical mechanics, in a short pulsed spatially periodic potential creates a situation of classical delta kicked rotor. Few examples like, a rotating permanent dipole in a pulsed field, a simple pendulum with gravitational field being switched on and off rapidly can be classified under the delta kicked rotor. The Hamiltonian for this system is:

$$H = \frac{P^2}{2m} + Kcos(\theta)\sum_n \delta(t - nT) \tag{2.44}$$

T is periodicity of kicks, K is the kicking strength. The parameter K can be 'tuned' to obtain various different dynamics in the phase-space.
In units of $m = 1$ and $T = 1$, the Hamilton's equations of the motion can be reduced to a set of mapping equations or maps. Since these are not the solutions that show the continuous time evolution, these are called mapping equations:

$$P_{n+1} = P_n + Ksin(\theta_n), \qquad \theta_{n+1} = \theta_n + P_{n+1} \tag{2.45}$$

The particles get a new set of moment distribution when the kicks are given and they evolve freely when the kicks are turned off. During the free evolution there is no change in momenta. These equations, in general, cannot be solved analytically. The parameter K plays important role in determining the dynamics. It can be seen from the following example, for $K = 0$ the phase-space will be very simple since θ_{n+1} gets very small increment from θ_n. And therefore, the advancement in l_{n+1} becomes very small from l_n. The classical phase space displays invariant curves. But when the value of K is larger than 5, θ_{n+1}, start getting maximum increment by $l_n + 5$ and the $sin(\theta_{n+1})$ gives any value between -1 to 1 randomly. Hence the dynamics is highly unpredictable and chaotic as can be seen in the Fig. 2.6.

There is another model similar to kicked rotor which is applicable in problems like many body system, *driven rotor*, where instead of potential being a sharp kick in time it oscillates in a sinusoidal fashion. Among the main real life problems, the dynamics of planets in the solar system is one of such examples.

2.6.2 Quantum Delta Kicked Rotor

The momentum evolution of particles when they are in quantum domain shows very different evolution as compared to that in the classical domain.

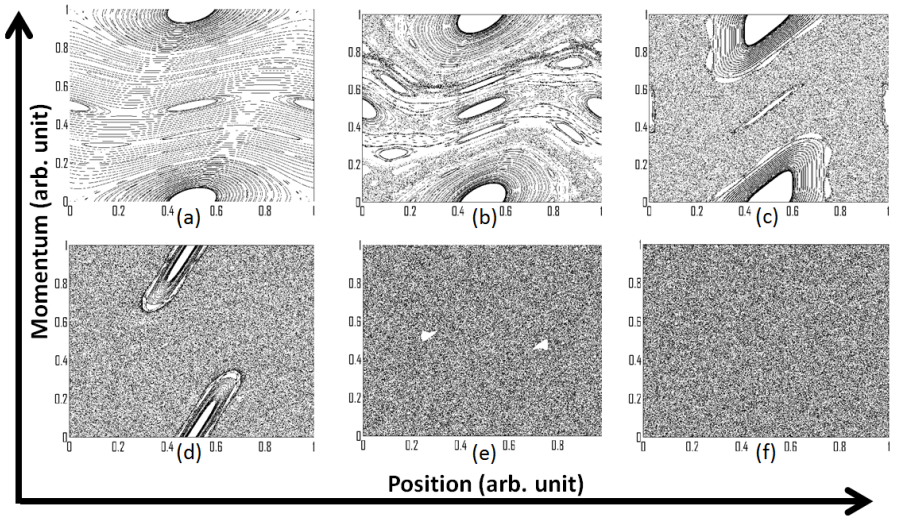

Figure 2.6: standard map of classical delta kicked rotor plotted with kick strength, K in the images (a) = 0.5, (b) = 1, (c) = 2, (d) = 4, (e) = 6 and (f) = 10. Transition from well predicted trajectory to completely random trajectory can be seen as the kick strength, K increases.

Particles evolve in lattice for certain small time and then they are left for free evolution. Therefore, the Hamiltonian is time dependent. In general, the solution of a time dependent Schrödinger equation is very difficult but when there is any symmetry in the Hamiltonian, the problem can be solved easily. In this particular case, the Hamiltonian:

$$H(t) = H_0 + V(t) \tag{2.46}$$

where, H_0 is the Hamiltonian of the system without the presence of the kicked pulses and $V(t)$ is the potential of due to the pulses. If the Hamiltonian would have been independent of time, the time evolution solution using the Schrödinger equation

$$i\hbar\frac{\partial\psi}{\partial t} = H\psi \tag{2.47}$$

would be:

$$\psi_n(x,t) = exp(-\frac{i}{\hbar}E_n t)\psi_n(x) \tag{2.48}$$

Though the Hamiltonian is time dependent, but the kicks are periodic in time, and therefore the potential term has time-translational symmetry, i.e $V(t+\tau) = V(t)$. This makes the problem little easier to be solved by using some trick [22]. Since, the Hamiltonian has time translation symmetry, it

is possible to find a set of eigenfunctions which simultaneously satisfies the eigenfunctions of time-translation operator, T_τ:

$$T_\tau \psi_n(x,t) = \psi_n(x,t+\tau) = \lambda_n \psi_n(x,t) \tag{2.49}$$

For the solution to be stationary, λ_n must be a pure phase factor,

$$\psi_n(x,t+\tau) = e^{-i\phi_n}\psi_n(x,t) \tag{2.50}$$

This follows that $\psi_n(x,t)$ can also be written as

$$\psi_n(x,t) = e^{-i\omega_n t} u_n(x,t) \tag{2.51}$$

where $u_n(x,t)$ is periodic in time, $u_n(x,t+\tau) = u_n(x,t)$, and $\omega_n = \phi_n/\tau$. Thus far the result followed only from the fact that the potential be periodic. The way wavefunction, $\psi_n(x,t)$ is expressed is exactly analogous to the wavefunction of a crystal lattice. These states are called *Floquet States* which is analogous to the *Bloch States*. By comparing Eq. 2.51 with the Eq. 2.48 we see that the role of energy in the Floquet system is taken by the so-called quasi-energy

$$\bar{E}_n = \hbar\omega_n = \frac{\hbar}{\tau}\phi_n \tag{2.52}$$

As the Floquet phase ϕ_n is defined only up to integer multiples of 2π, quasi-energies are defined only up to integer multiples of h/τ. This is quite analogous to a similar phenomenon that is observed in a real lattice; the formation of Bloch state gives rise to the possible wavenumbers are integer multiples of the reciprocal lattice vectors. As a consequence, the wavenumbers can be limited to the first Brillouin zone. An equivalent Brillouin zone is taken in the Floquet system in the range between $[-h/2\tau, h/2\tau]$. This shows many similarities between a crystal and a quantum system with time oscillating potential.
Time evolution operator $U(t)$ is defined as :

$$\psi(x,t) = U(t)\psi(x,0) \tag{2.53}$$

using this equation in the time dependent shcrödinger equation, we get:

$$i\hbar\dot{U} = HU \tag{2.54}$$

It can easily be shown that the time evolution operator U is unitary.

$$U^\dagger U = 1 \tag{2.55}$$

At $t = \tau$ the time evolution is

$$\psi(x, \tau) = U(\tau)\psi(x, 0) \tag{2.56}$$

The more generalized form can be written as

$$\psi(x, n\tau) = [U(\tau)]^n \psi(x, 0) \tag{2.57}$$

Therefore, the time-evolution operator which follows

$$U(n\tau) = [U(\tau)]^n \tag{2.58}$$

It is sufficient to just know the operation of $U(\tau)$ to understand the wave function at any stroboscopic time, $n\tau$. Since, U is unitary matrix, it can be diagonalized by unitary transformation such that,

$$U = V^\dagger U_D V \tag{2.59}$$

where, U_D is diagonal matrix, and V is another unitary matrix. The eigenvalues of the evolution matrix, U will be the diagonal elements of the diagonal matrix, U_D.

$$(U_D)_{nn} = e^{-i\phi_n} \tag{2.60}$$

The study of Floquet system has reduced to the study of the eigenphases of $U(\tau)$.

For a kicked system, the time during which the potential is switched on is very small and it can be treated as delta function. Using a general potential, the Hamiltonian,

$$H(t) = H_0 + V_0 \sum_n \delta(t - n\tau) \tag{2.61}$$

Assuming the delta function to be of a form with on-time $\Delta\tau$ and the potential height $(\Delta\tau)^{-1}$, the Hamiltonian will of this form:

$$H = \begin{cases} H_0 & n\tau < t < (n+1)\tau - \Delta\tau, \\ H_0 + \frac{1}{\Delta\tau} V_0 & (n+1)\tau - \Delta\tau < t < (n+1)\tau \end{cases} \tag{2.62}$$

The Hamiltonian is piecewise constant, the time-evolution operator $U(t)$ can be obtained by direct integration. For $0 < t < \tau - \Delta\tau$ we have,

$$U(t) = exp(-\frac{i}{\hbar} H_0 t) \tag{2.63}$$

and for $\tau - \Delta\tau < t < \tau$

$$U(t) = exp[-\frac{i}{\hbar}(H_0 + \frac{1}{\Delta\tau} V_0)(t - \tau + \Delta\tau)] U(\tau - \Delta\tau) \tag{2.64}$$

The Floquet operator,$F = U(\tau)$, which is obtained by setting t= τ is

$$F = exp[-\frac{i}{\hbar}(H_0 + \frac{1}{\Delta\tau}V_0)\Delta\tau]exp(-\frac{i}{\hbar}H_0(\tau - \Delta\tau)) \tag{2.65}$$

which further simplifies when the pulse on-time $\Delta\tau \to 0$

$$F = exp(-\frac{i}{\hbar}V_0)exp(-\frac{i}{\hbar}H_0\tau) \tag{2.66}$$

The delta kicked rotor is an example where the potential, $V_0 = kcos(\theta)$. Then the Floquet operator,

$$F = exp(-\frac{i}{\hbar}kcos(\theta))exp(-\frac{i}{\hbar}\frac{\tau}{2}L^2) \tag{2.67}$$

where, $H_0 = L^2/2$ with L being the angular momentum operator. In the eigenbasis of L,

$$|n\rangle = \frac{1}{\sqrt{2\pi}}e^{in\theta} \tag{2.68}$$

The matrix elements of F are given by

$$\begin{aligned} F_{mn} &= \langle n|F|m\rangle \\ &= \frac{1}{2\pi}\int_0^{2\pi} e^{-in\theta}exp(-\frac{i}{\hbar}kcos\theta)exp(-\frac{i}{\hbar}\frac{\tau}{2}L^2)e^{im\theta}d\theta \\ &= exp(-\frac{i}{\hbar}\frac{\tau}{2}m^2)\frac{1}{2\pi}\int_0^{2\pi} exp(-\frac{i}{\hbar}kcos\theta)e^{i(m-n)\theta}d\theta \\ &= exp(-\frac{i}{\hbar}\frac{\tau}{2}m^2)i^{m-n}J_{m-n}(\frac{k}{\hbar}) \end{aligned}$$

Where, J_m is Bessel function of order m. The value of Bessel function decreases as the order increases, therefore the off-diagonal elements of the Floquet operator goes to smaller and smaller as compared to the diagonal elements. With the given matrix element, the energy eigenvalues can be calculated. Assume, at time, $t = 0$ the probability amplitude of finding the rotator at an angle θ be $a(\theta)$. The components of the state vector

$$A_0 = \begin{pmatrix} a_1 \\ a_2 \\ a_3 \\ : \end{pmatrix} \tag{2.69}$$

in the basis of eigenfunctions of $L$are obtained by Fourier transformation

$$a_n = \frac{1}{2\pi}\int_0^{2\pi} a(\theta) d^{-in\theta} d\theta \tag{2.70}$$

The state vector after Nth kick

$$A_N = F^N A_0 \tag{2.71}$$

The expectation of the energy eigenvalue of the kicked rotor can be calculated after N_{th} kicks:

$$\begin{aligned} \langle L^2 \rangle &= A_N^\dagger L^2 A_N & (2.72)\\ &= \hbar^2 \sum_{l,m,n} l^2 (F^N)_{lm} (F^N)^*_{ln} a_m a_n^* & (2.73) \end{aligned}$$

The average energy is calculated using numerical simulation and plotted as a function of number of kicks. There is big difference between the energy growth of the classical system and that of the corresponding quantum system. The energy gets saturated (see fig. 2.7) in the case of quantum system, whereas it keeps on increasing for the classical system. This difference makes the kicked rotor very sensitive tool to measure effects of decoherence in the system, because decoherence leads to make the system behave as a classical system. In addition, since we are using ultra-cold atoms in standing wave, the tunability of various parameters, such as addition of noise with certain correlation, will show up in the mean energy growth plot. Another way of understanding the phenomena of saturation in energy is through the crystal analog of the kicked rotor. A crystal with added impurity makes either the periodicity or the potential at each lattice site random. Under this noisy environment, the wave function of electrons start interfering such that the probability amplitude is maximally localized near the lattice sites as a consequence a conductor becomes insulator in such environment. This phenomenon in a crystal is known as 'Anderson Localization' [23]. Analogous to that, in a kicked rotor, the momentum starts getting localized at certain values. Atoms do not occupy all the momentum states. As a consequence, the energy, which is a contribution from all the available momentum distribution, does not increase linearly with kicks.

2.6.3 Levy-Kicked Rotor

Thus far, the pulses of optical lattice potential were given with a constant periodicity which shows the phenomenon of dynamical localization which

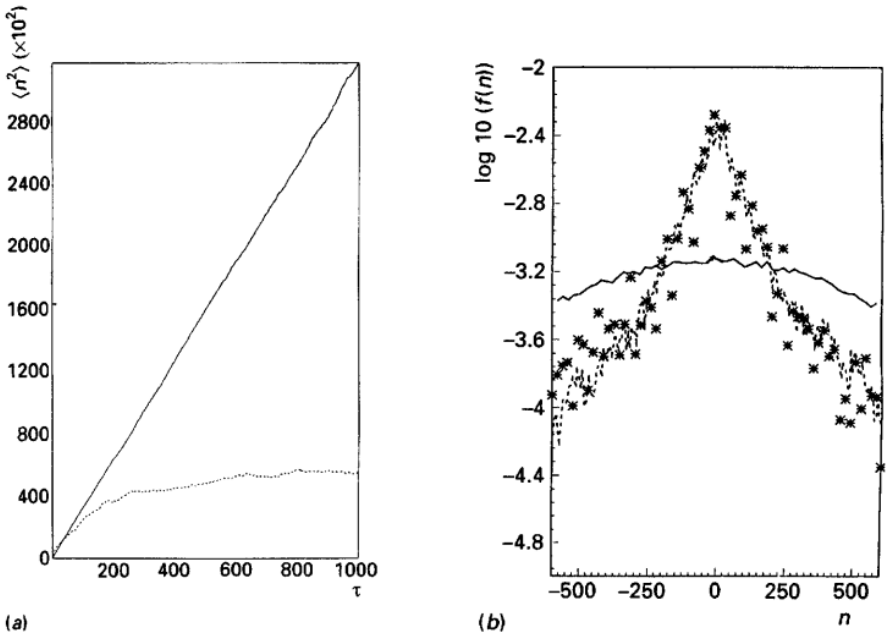

Figure 2.7: (a) classical and quantum diffusion for the kicked rotator for k =5. The averaged energy $\langle n^2 \rangle$ is plotted versus number of kicks (in the units of τ). (b) Classical and quantum momentum probability distribution after 1000 kicks. For the stars see the original work in the ref. [15]

is a pure quantum effect. Unavoidable coupling of a system with environment leads to suppression in interference phenomena which results a classical system. The rate at which this transition happens is described by a decoherence factor which has a form $D(t) = D(0)exp(-t/t_c)$. The decoherence time, $t_c = 1/[m\kappa(\Delta x)^2]$ depends on the mass, m of the particles, the coupling strength, κ and the spatial separation of the interfering states, Δx. Many experiments have been performed to verify the exponential time dependence of the de-coherence factor by changing either of the terms on which decoherence time, t_c is dependent upon. Experiments with cold atoms has been performed [18, 16] in which by controlling the amplitude of resonant light, the coupling with environment, κ can be controlled. Effectively, this noise modifies the kick strength, k with an additional noise in it which induces decoherence to make the system more classical, i.e, describable by classical equations of motion. This can be understood as follows: In the absence of noise, the quasi-energy eigenstates of the Floquet operator, F are exponentially localized. As the noise is added, it leads to coupling between the quasi-energy eigenstates which results transition between them. In another approach, where the pulses do not remain strictly periodic as some noise is added to it, the result could be very different[19]. In this thesis, the theoretical work done for this particular case is considered as a main focus and the aim is to experimentally verify.

The non-periodicity in the kick sequence can be obtained using a suitable waiting time distribution which asymptotically follows power law distribution, $w(\tau) = \tau^{-1-\alpha}$ [19]. This kind of distribution, in general, is classified as Levy-statistics. In this particular experiment, the control over α allows to tune the Levy distribution and to observe its consequences. In other past experiments with kicked rotor system this particular kind of tunability was never performed. The average waiting time, $\tilde{\tau} = \int_0^\infty d\tau\tau w(\tau)$, plays important role to tune fully coupled situation (large α) to isolated situation (small α).

For $\alpha \leq 1$ the mean waiting time, $\tilde{\tau}$ becomes infinite which alters the decoherence from its well-known exponential distribution. In this sense, the de-coherence rate becomes ill defined.

It is worked out (see [19]) for Levy noise with asymptotic power-law distribution, $w(\tau) = \tau^{-1-\alpha}$ in the two different range of the value α which shows some remarkable results. For $\alpha > 1$, the decoherence function, $D(t,0) = exp[-|t|/(\tilde{\tau}t)]$, still follows an exponential form. However, the effective coherence time is modified to $\tilde{\tau}t$ which increases as α decreases to 1.

While on hand, for the value of $\alpha < 1$, the decoherence function

$$D(t,0) = E_\alpha(t^\alpha/[\Gamma(-\alpha)ct_c]) \tag{2.74}$$

where, $E_\alpha(z) = \sum_{n=0}^{\infty} z^n/\Gamma(\alpha n + 1)$ is Mittag-Leffler function. The expansion of the function, $E_\alpha(z)$, shows a stretched exponential form, $D(t,0) = exp[t^\alpha/(\Gamma(-\alpha)ct_c)]$, while for large times it crosses over to the power law $D(t,0) = (ct_c/\alpha)t^{-\alpha}$. By tuning the value of α, the functional form of decoherence factor can be modified which can be reflected in the variance of momentum diffusion of the kicked rotor.

$$var(p(t)) = \frac{D^* t^*}{t_c} \frac{sin\pi\alpha}{\pi c} t^\alpha \tag{2.75}$$

The variance of momentum, $var(p(t))$ for different α and noise strength,κ are plotted in the fig. 2.8. In this, noise strength, $\kappa = \bar{k}_n^2$ is defined as the variance of the perturbation, k_n in the kicking strength.

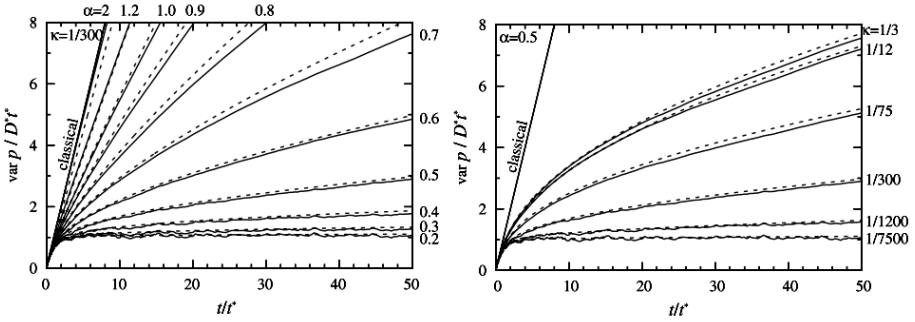

Figure 2.8: In the left panel, α is varied while the noise strength $\kappa = 1/300$ is fixed. In the right panel, the result is for fixed $\alpha = 0.5$ and varied noise strength κ. The dashed curves are the theoretical prediction whereas the solid curves are numerical simulation [19].

Chapter 3

Experimental Methods

Advancement in technologies such as precise control, better vacuum systems, stabilized lasers has opened up a new area of research with ultra-cold atoms. In the previous chapter, we have understood the theoretical background for trapping atoms and cooling them down to temperature of order few μK. The condition desired for these experiments are very extreme as the system is highly sensitive towards any interaction with the environment. This chapter discusses the various technical requirements and their arrangements for the experiment with ultra-cold atoms. Few of such important needs are ultra-high vacuum, stable laser system, precise control over laser beams and magnetic field.

3.1 Vacuum System

One of the most important needs, for trapping atoms of very low temperature, is to isolate the atoms from rest of the environment. This is because the background particles can transfer enough momentum to the trapped atoms to overcome the trapping potential.

In the fig. 3.1, source of Rb atoms is connected to the left most part. The Rb container is heated up to 70 ^{o}C, this starts the production of Rb vapor which emits through the collimator tube. The 'elbow' connected to the left end of the collimator is set up to a temperature 120 ^{o}C, which decides the rms velocity of the atoms. This temperature is tuned for fast loading with our Zeeman slower. To thermally isolate the oven from rest of the assembly, we placed a glass isolator with the conflat flange (CF-35) opening. At the right-side opening of the collimator we have installed a copper cup-like structure which has a small hole in the center through which atoms go to the next part of the assembly. The copper cup is connected to an

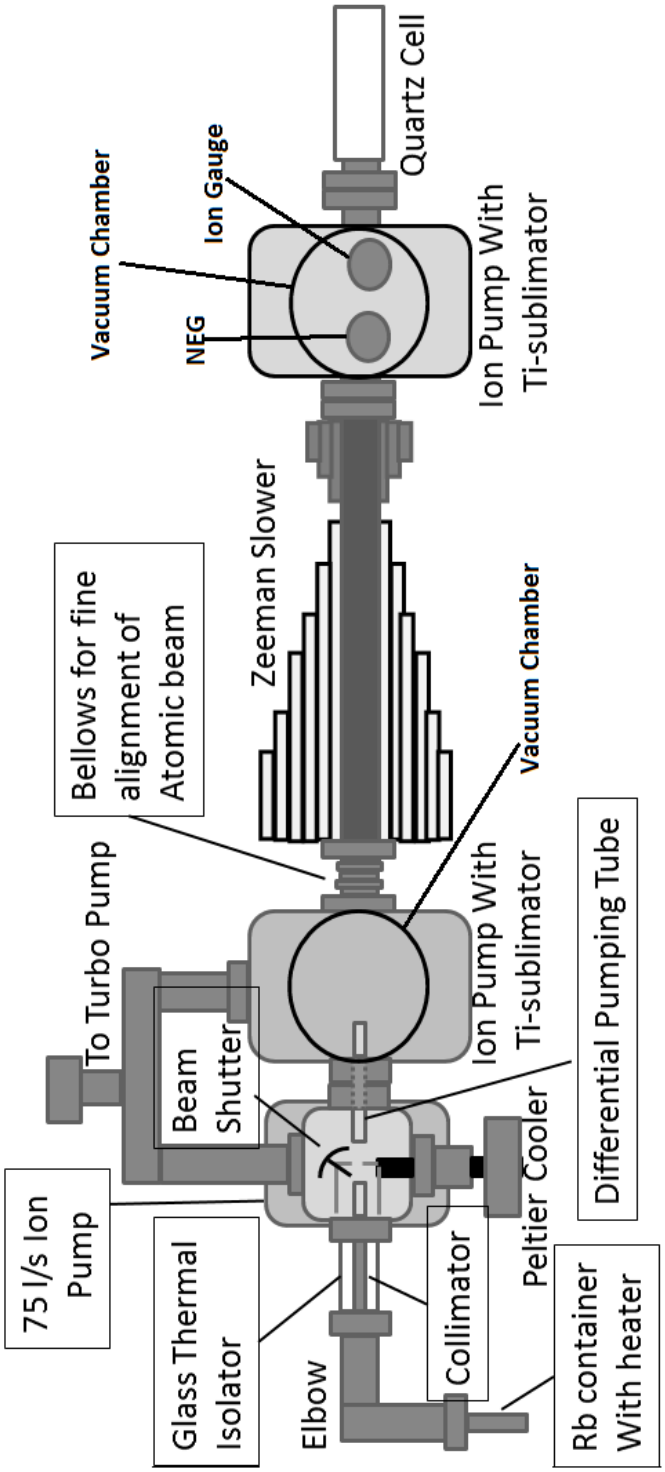

Figure 3.1: A schematic diagram of the vacuum system for trapping Rb atoms

electric feed-through whose outer terminal is connected to a peltier cooler. The temperature is kept at -25 ^{o}C. Because of high thermal conductivity of copper, the temperature of the cup is also the same. The purpose of keeping it cool is to seize the movement of the atoms coming out of the collimator which are not collimated. As these atoms hit the copper wall, they mostly stick to the wall because of low temperature. And because of this, beam of Rb atoms with very good collimation is obtained at the quartz cell. At the other side of the copper cup, a pneumatic actuator controlled beam shutter is installed. This is helpful to avoid any unwanted inflow of Rb atoms to the quartz cell, when not needed. A differential pumping tube is connected between the 'six-way cross' and the vacuum chamber connected to Zeeman slower. The differential pumping tube acts as a 'resistor' in an equivalent electrical circuit. It balances a pressure difference at the two openings.The smaller inner diameter and relatively longer length increases the range of the pressure difference that needs to be balanced as it can easily be understood from the electrical analog. This is necessary because the pressure in the 'six-way cross' is higher because of uncollimated Rb atoms, than the vacuum chamber which is attached to an ion pump. The order of pressure in the 'six-way cross' is below 10^{-8} Torr whereas that in the vacuum chamber is below 10^{-10} Torr. Atoms after passing through the differential pumping tube enter a long tube (80 cm) which is wound with specially designed layer of coils to produce field needed for the Zeeman slower which will be discussed in the next section. Another chamber is connected to the end of this tube. Another ion pump is attached to this chamber to ensure the pressure to be less than the desired from inside the quartz cell. Obtain atoms with low speed to the final destination i.e the quartz cell, is the ultimate aim. Once the atoms are there inside the cell, such MOT, magnetic trap etc. are used to manipulate atoms. In the following subsections, little more technical details of the important parts are discussed.

3.1.1 Vacuum Pumps and Assembly

The vacuum needed for trapping atoms in MOT and magnetic trap requires ultra-high vacuum. Collision from 'hot' atoms can lead to loss in the quantum state of specially prepared atoms. Pressure below 10^{-10} Torr is considered to be good for such high precision experiments. To create such high vacuum and maintain for longer time vacuum pumps of certain class are needed. In general, the pumps which work on the mechanism based on mechanical pumping, for example scroll pump, do not work pressure below 10^{-4} Torr. Turbo pump, on other hand, is one of such mechanical pumps works in the much lower pressure range (below 10^{-9} Torr). But, it cannot maintain such

high pressure difference, so in many applications the high pressure side of the turbo pump is connected to a rotary pump and the net pressure difference across the turbo pump is reduced to 10^{-6} Torr. This combination is pretty standard and such stand-alone pumping stations are provided by many vendors.
The pumping station needs to be connected to the vacuum assembly to pump out of the gases that are already inside the assembly. Initially the pressure falls rapidly, which later starts becoming slower. We kept the pump continuously running for two days, we found the pressure gets saturated to the order $10^{-}9$ Torr. At this stage, further decrease in pressure becomes very difficult. The trick now one needs to play is to heat the whole system. This will increase the pressure and release the molecules which are attached to the inner surface of the vacuum assembly. The throughput speed of a pump, which is defined as the rate at which the amount of particles is thrown out from a chamber, is proportional to the pressure inside. Therefore this leads to increase in rate of pumping out of the unwanted particles from the chamber. To heat the whole assembly, we wrapped glass wool coated heating tapes on the whole system. Special care had been taken near the quartz cell since it is sensitive to rapid temperature change and steep gradient in temperature. We covered the complete quartz cell with an aluminum hollow cylinder and the heating tapes were wrapped over it. The air inside, as it gets hot, heats up the quartz cell with very slow rate in a homogeneous manner. Care had also been taken near the glass isolator by padding thick layer of aluminum foil. The current in the heaters were increased slowly to ensure slow heating rate. As the temperature starts increasing sudden increase in pressure had been observed indicating that the particles sitting at the surface were getting released. To monitor the pressure and temperature, we connected temperature sensors to a computer using DAC card and made a program in Labview to display. Once, saturation in pressure was observed we increased the current in the heaters slowly. We repeatedly kept increasing the current in the heater till the final temperature reached to 250 ^{o}C which took us about 3 days. We kept the whole system in this condition for one more day, the pressure went below 10^{-9} Torr. At the same condition, we turned on various other pumps, such as the ion pumps, Ti- sublimator pumps, non-evaporable getter pumps (NEG) that was installed in the vacuum assembly. These pumps operate at pressure below 10^{-8} Torr which is meant for continuously keeping the pressure inside the chamber reduced. When sufficient amount of current is flown through a Ti-sublimator pump, it releases vapor of titanium which coats the inner wall of the chamber which has a tendency to adsorb particles which come into contact. NEG, again, works on similar principle of adsorption but it does not evaporate any material. Instead, it's internal structure is such

that it has very large surface area exposed inside the vacuum system. Ion pumps work by ionizing the particles and forcibly dumping them on a surface of titanium which absorbs them. We have connected three Ion pumps at different positions as can be seen in the fig. 3.1. Once these pumps were activated, we observed, again, increase in pressure for a moment. This could be because of the particles from the surface of these pumps would have released. We slowly started reducing the temperature. The pressure kept on decreasing and at room temperature the pressure went down to below 10^{-11} Torr.
Prior to starting the pumping out process, while assembly of the system, we took good care of cleaning of each and every component needed for the vacuum system. All the inner wall of the vacuum chambers and the tubes were cleaned using the three chemicals, iso-propanol, acetone and ether. The smaller components were first sonicated with acetone and then further cleaned with the above mentioned three solutions. Quartz cell was cleaned with dilute hydrofluoric acid (HF), which had got a thin layer of titanium coating inside, earlier. A glass ampule containing Rb atoms inside was placed in a machined copper pinch off tube. The inner diameter of the pinch-off tube was kept slightly larger than the glass ampule so that it just fitted well. The open end of the tube was sandwiched between knife-edge conflat flanges.
Once the vacuum of desired pressure was obtained, we gently crushed the pinch-off tube to break the glass ampule to eject Rb atoms. To detect the atomic beam, we sent a laser of frequency closely scanning to one of the transition lines and observed the spectrum. We also tested the working of beam shutter as we closed the shutter, no signal was measured.

3.2 Lasers and Optics

Despite that Rb being one of the most simple structures, there are couple of transition lines that needs to be taken into consideration while trapping them in MOT or for further experiments. Coupling of orbital angular momentum with the spin angular momentum of the outer electron gives rise to the fine structure lines (doublet). Furthermore, coupling with the nuclear angular momentum splits the line into so called hyperfine structures denoted by **F**. These hyperfine states further gets split into certain number of sublevels for a given **F** state when a magnetic field is applied.

$$\mathbf{F} = \mathbf{J} + \mathbf{I} = \mathbf{L} + \mathbf{S} + \mathbf{I}$$

where, **L** and **I** are orbital angular momentum and spin angular momentum respectively. The transition rules are following:

$$\Delta \mathbf{F} = 0, \pm 1 \tag{3.1}$$
$$\Delta m = \pm 1 \tag{3.2}$$

where, m_f is magnetic quantum number and takes values $m_f = -F, -F+1, -F+2.....F-2, F-1, F$. For spontaneous emission, the change in magnetic sublevels is, additionally, by $\Delta m = 0$.
For our experiment we have used laser frequency slightly red detuned to $\mathbf{F = 2}$ to $\mathbf{F' = 3}$ transition for the MOT and the Zeeman slower beams (see fig. 3.2). This transition transition cycle is closed as once the atoms get excited they can only come back to $\mathbf{F = 2}$ state only, because the other state $\mathbf{F = 1}$ is forbidden by selection rule. And therefore, atoms remain tuned to the laser frequency which is very helpful for continuously forcing them. But, in addition to this process, atoms get excited from state, $\mathbf{F = 2}$ to the state, $\mathbf{F' = 2}$ also, because of scattering from off-resonant light. Though, the rate is low, but it is there and it scales as intensity of light. And from this state atoms also relax to $\mathbf{F = 1}$ state by spontaneous emission. After a number of cycle, atoms would end up occupying $\mathbf{F = 1}$ state and they will no longer be in resonance to the main beam. The trapping potential will be vanished. To eliminate this issue, another beam which is slightly red detuned to $\mathbf{F' = 1}$ to $\mathbf{F = 2}$ transition line is shone (see fig. 3.2). The excited state atoms also decay to $\mathbf{F = 2}$ which is the favorable state for our experiment. By this mechanism the $\mathbf{F = 2}$ starts getting repopulated again. This process is known as re-pumping and the laser beam is called 'repump beam'. The rate at which repumping is needed should be just higher than the rate at which atoms go to $\mathbf{F = 1}$ state due to the off-resonance scattering rate. And therefore, the power needed for repumping beam is very low for this reason, the effect of repump beam on the atoms, otherwise, is negligible.

3.2.1 Laser Locking

As discussed, the frequency of laser needs to be stable and tunable over a range of few 100's of MHz. Diode lasers are pretty good for this purpose. A complete setup of laser consists of laser diode coupled with a cavity. The cavity is generally made with the help of grating. The angle of the grating is controlled by a piezo actuator due to which the frequency is tuned with accuracy better than a MHz. By applying DC voltage to the peizo, the length of the cavity can be varied and hence the frequency can be changed. The voltage can even be made oscillating, which will generate laser beam with

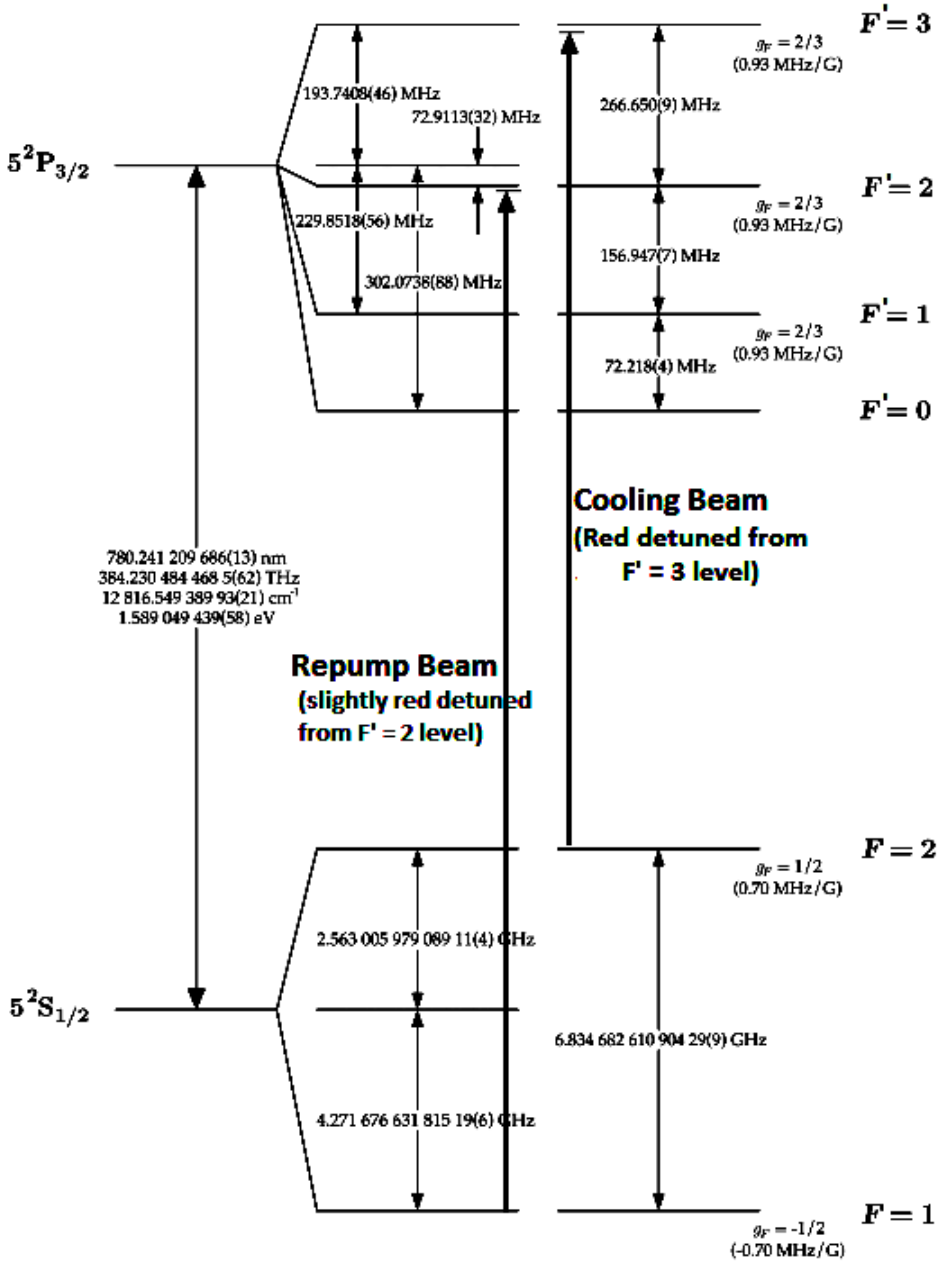

Figure 3.2: D2 energy level diagram of Rb87 atoms [24, 25]

scanning frequency. This is very important while observing spectrum of a given atoms.

To produce laser of frequency exactly matching with the transition lines, a reference is needed for which we use a cell filled with Rb atoms. In a natural source, the two isotopes of Rb-85 and Rb-87 are found with abundance 72.8% and 27.8%, respectively. By changing the DC voltage and the scan range on the piezo, absorptions peaks of the Rb atoms are detected. The detected peaks are only from the D1 and D2 transition lines of Rb-85 and Rb-87 this is because at room temperature the broadening in the spectrum due to Doppler effect caused by the randomly moving atoms is larger than the frequency separation between the hyperfine lines. We use a technique called saturation absorption spectroscopy to get rid of broadened spectrum. The laser beam is reflected from a thick glass cell. The two surfaces reflect two parallel beams of nearly same intensity which are allowed to pass through the Rb glass cell. Two photo-diodes are placed in front of the two beams and a difference signal is observed on an oscilloscope. When the output voltage of the two photo-diodes and the intensity of the two beams are same, a flat signal is expected. Another beam, with more power, is shone from the opposite direction which overlaps with one of the two beams at a very small angle which can be assumed to be counter-propagating. A group of atoms with zero velocity do not see any difference in the frequency of the two opposite beams. Since, the laser frequency is scanning at an instant when the frequency matches to one of the transition line the two opposite beams excite the atoms with zero velocity class. And because the opposite moving laser is more powerful, the number of atoms left in ground state is very less therefore the beam falling on the photo-diode doesn't get absorbed much. Whereas the other beam (with no counter-propagating light) gets absorbed by the atoms of zero velocity class. This creates a peak in the difference signal. The line width is much narrower than the hyperfine splitting and there should be three peaks for each of the D1 or D2 lines. But, on the scope we see three more intense peaks which are result of cross-over resonances. A class of atoms moving towards one of the beams will see positive shift in frequency, while the same atoms will see a negative shift in frequency for the opposite beam. If it so happens that the positive shift and the negative shift matches two different hyperfine transition lines then there will also be some peaks corresponding to this frequency which happens to be at the center frequency of each pair of two hyperfine transitions.

Once the reference is set, the laser needs to be locked to the peak which satisfies our requirement. This is done by modulating the laser-frequency at very high frequency with small amplitude. The signal from the SATABS is demodulated with the reference frequency which generates an error signal and

it is sent back to the piezo crystal for feedback. This process is known as lock-in detection. When the laser frequency drifts, the error signal is generated in such a way that it drives the peizo to compensate for the drift. Once the lasers are locked to the peaks, using acousto-optic modulators (AOM) the frequency of the laser beams are further modified with an accuracy of few units of MHz.

3.2.2 Optical Setup

The power needed for the experiment is obtained from two different lasers. One of them (high power laser) is locked to $\mathbf{F = 2 \rightarrow F' = 2}$ transition line and the other to $\mathbf{F = 1 \rightarrow F' = 1}$ transition line. The frequency needed for the MOT and the repump beams are different from the frequency where lasers are locked. This is because of certain limitations with acousto-optic modulators (AOM) since in general, they operate with good amount of deflection at the frequency of order few 10's of MHz. Therefore, locking to $\mathbf{F = 2 \rightarrow F' = 3}$ is not useful when the detuning needed is of order few MHz. The frequency of the laser is upshifted using AOMs in double pass configuration (see fig. 3.3). This configuration also ensures that while shifting the frequency, the coupling of light to the fiber doesn't go bad. The AOM for the MOT beam is operated at 128 MHz, which means that the detuning from the $\mathbf{F = 2 \rightarrow F' = 3}$ transition will be $\Delta = 266.65 - 2 \times 128 = 10.65$ MHz. For MOT repump beam, the AOM is operated at 76 MHz, the corresponding detuning will be $\Delta = 156.95 - 2 \times 76 = 4.95$ MHz. Inside an AOM a crystal is exerted strain by a piezo at a given frequency which creates a traveling wave of density inside the crystal. This acts as traveling grating and once light at proper angle is shone it adds up or subtracts that frequency from the AOM, as can be understood by the process of photon-phonon interaction. Also, the output light which is frequency-shifted exits at different angle which gives an advantage of spatial isolation. All the laser beams are taken to the table which consists of the vacuum assembly using optical fibers. The beam for the MOT is sent to a six-way beam splitter, from where the six beams are aligned as can be seen in the fig 2.3, around the quartz cell with proper polarization. The fiber for the Zeeman slower beam, which contains both the main beam as well as the repump beam, is sent from the front part of the quartz cell passing through the Zeeman slower tube till the end of the differential pumping tube. The repump beam of the Zeeman slower is also used for the MOT repump beam, since the detuning is not very different for both of them. We have two more set of beams prepared, imaging beam and optical pumping beam. The imaging beam is used after the atoms are loaded and experiments are performed. While imaging, two

short pulses of light are shone which passes through the atomic cloud and falls on an EMCCD camera. At the same time the camera is given a trigger to capture the images. One more image is taken without the imaging beam for background reference. The laser for the optical pumping is used when the atoms are transfered to magnetic trap where a particular magnetic sublevel can only be trapped. Before transferring atoms to the magnetic trap, a mild homogeneous magnetic field is turned on with the optical pumping beam. This beam is exactly tuned to $\mathbf{F = 2 \rightarrow F' = 2}$ state. As discussed in the theory chapter, this beam, for a given direction of magnetic field pumps the atoms to either $m_f = -2$ sublevel or $m_f = +2$ sublevel. By flipping the field we pump all of them to the desire sublevel, i.e $m_f = +2$.
Optimized coupling to fibers and AOMs are very important to obtain sufficient power at the output. As the output beam of a laser has beam width around 2mm, the beam diameter is made narrow by using a pair of lenses in a telescope configuration. This is to ensure that majority of the power of the beam passes through the opening of an AOM and fiber coupler. Additionally, near the focus point we have placed mechanical shutters to block the beams completely (not shown in the figure to avoid complexity) to make sure that there is complete blocking of light during magnetic trap. Once, the beam is sent through an AOM, generally, in the output we get two beams deflected at certain angle. One of them is unshifted beam, and called as zeroth order beam, the other one is either +1st order or -1st order depending upon the upshift or downshift in frequency. To make the output beams parallel a lens inserted at a distance from the AOM equal to its focal length. This ensures that when the frequency is changed the direction of the shifted beam does not change. A mirror is placed to reflect the beams back to the AOM for double pass. The position of the mirror is also at the same distance, the focal length 'f', away from the lens because the incoming beams do not remain collimated as they pass through a lens, so, after traveling '2f' ,after reflection, become collimated when they pass through the lens back. The retardation plates ($\lambda/2$ waveplates) are used for rotating the plane of polarization. It is very important when the beam passes through a polarizing beam splitter cube to balance the power of the two beams. This is important while coupling in the optical fibers, because the fibers are polarization maintaining single mode so the polarization needs to be matched.

3.2.3 Imaging

After the atoms are loaded in MOT and then further experiments are performed with it the only information we get from the atoms is by imaging them. Various methods have been implemented for imaging the cloud. One

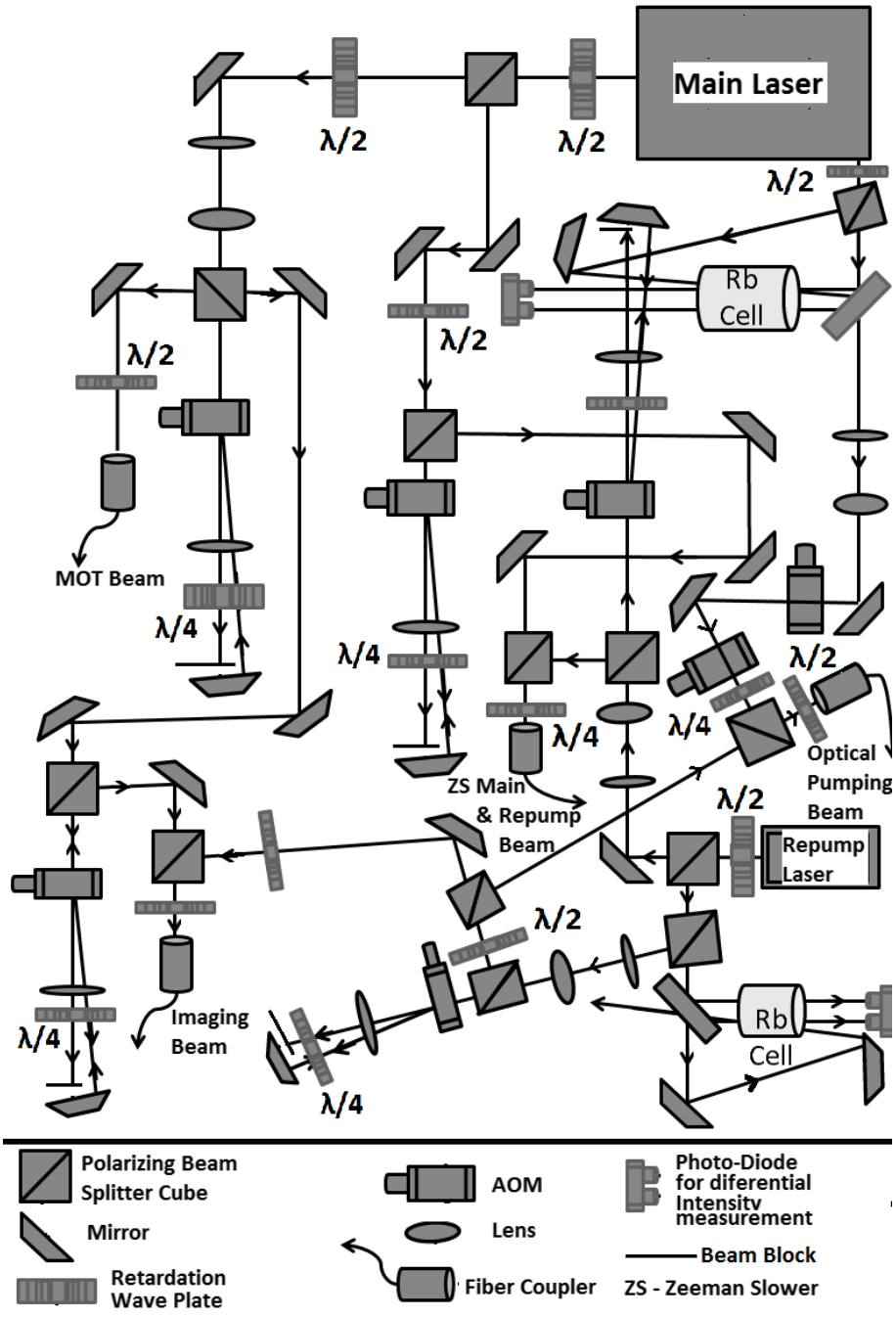

Figure 3.3: Optics arrangement on the optics table

of them is the absorption imaging, which relies on the fact that the amount of light being absorbed increases when more atoms come in the path. While imaging, a collimated beam of light is passed through the cloud which falls on the camera sensor (fig. 3.4). This is a one-to-one imaging where the two lenses are of same focal length so the cloud size does not scaled. The purpose of iris is to block the light coming from the fluorescence of the atomic cloud to get well resolved signal.

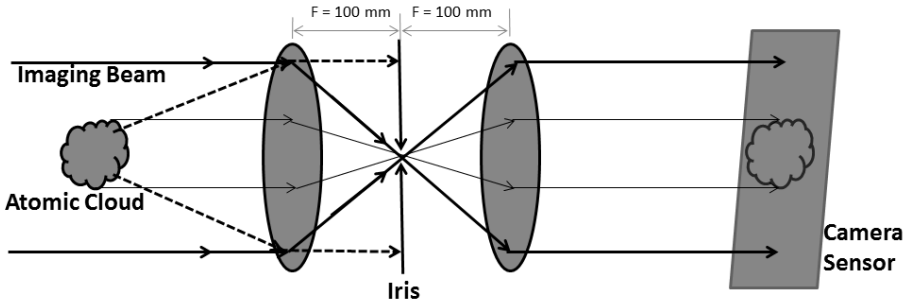

Figure 3.4: schematic of imaging beam setup

It maps the 2 dimensional density distributions of the atoms. For low power, it follows from the Lambert-Beer's law:

$$\frac{dI}{dz} = -\sigma I \tag{3.3}$$

therefore,

$$I = I_0 e^{(-\sigma z)} \tag{3.4}$$

where, σz is optical density σ is scattering cross section
To extract the information only from the cloud, we take three images; one with atoms,I, one without atoms, I_0 and the third without imaging beam, I_b turned on. The last image compensates for any possible dark current in the camera or, any other background light. The optical density of the cloud can be extracted out from these three images as:

$$OD = ln\frac{I_0 - I_b}{I - I_b} \tag{3.5}$$

The main beam used for imaging is used from the main laser which is locked to $\mathbf{F = 2 \rightarrow F' = 2}$ state. The frequency is further upshifted using an AOM and is closely tuned to $\mathbf{F = 2 \rightarrow F' = 3}$ state. In addition, a repump beam is also shone to avoid loss of atoms from the desired state while imaging. The duration of the pulse is very short ($\sim 50\mu s$) to avoid any possible drift

of the atoms during imaging. Since the resonance light is used for imaging, the atoms after this step gets kicked out and they no longer remain there after certain time. We shine another imaging pulse after 200 ms. This image only captures the intensity distribution of the imaging beam. Another image is taken after the same time delay, 200 ms, without turning on the imaging beam. The processed images reveal various interesting outcome which includes temperature, momentum distribution etc. To measure the momentum distribution, images after two different time of free evolution of the cloud is taken; this time is popularly known as time-of-flight (TOF). By comparing the evolution in the cloud size, momentum distribution can be extracted out. Assuming, the cloud to be gaussian, the rate at which the standard deviation changes for two different time-of-flights, the temperature is estimated. Other information, like formation of BEC, vortex formation which depends on the shape of the cloud after free evolution are also obtained from the imaging.

3.2.4 Optical Lattice

A laser is coupled through a fiber and the output is attached to a collimator. The collimated beam is then reflected back using a mirror to create optical lattice. To ensure that the path exactly matches, the reflected power should be coupled to the fiber. Adjusting the wave-plate orientation, certain fraction of the reflected light after passing through the beam splitter cube falls on the photo-diode. The fine adjustment of the mirror is made by maximizing the voltage of the photo-diode. To verify that the beam is passing through the atomic cloud, the laser is tuned closer to the Rb transition lines. The mirror is blocked, due to which it forms traveling wave. If this beam is aligned to the cloud, it kicks them away. And then by unblocking the mirror, which creates standing wave, the position of the atoms does not get shifted a lot. The AOM is driven at 120 MHz, by a 2 Watt RF amplifier. The input RF signal passes through a voltage controlled switch, which is operated by a function generator to create desired number of kicks with the required pulse width. The laser beam after the exit of the laser source passes through a telescope, to reduce beam diameter, before entering into the AOM. The rise and fall time is limited, also, by the beam width because as the beam travels inside the crystal, the acoustic wave inside the crystal takes some time to travel across the beam diameter. And for this reason, if the beam diameter is larger, the longer will it take to switch the laser beam. We have used 150 mW total output laser, which, at the output of the beam collimator we get 70 mW power. Corresponding to this power, the trap depth is of order 100's μK at 1GHz detuning. The frequency is stabilized by the stable current

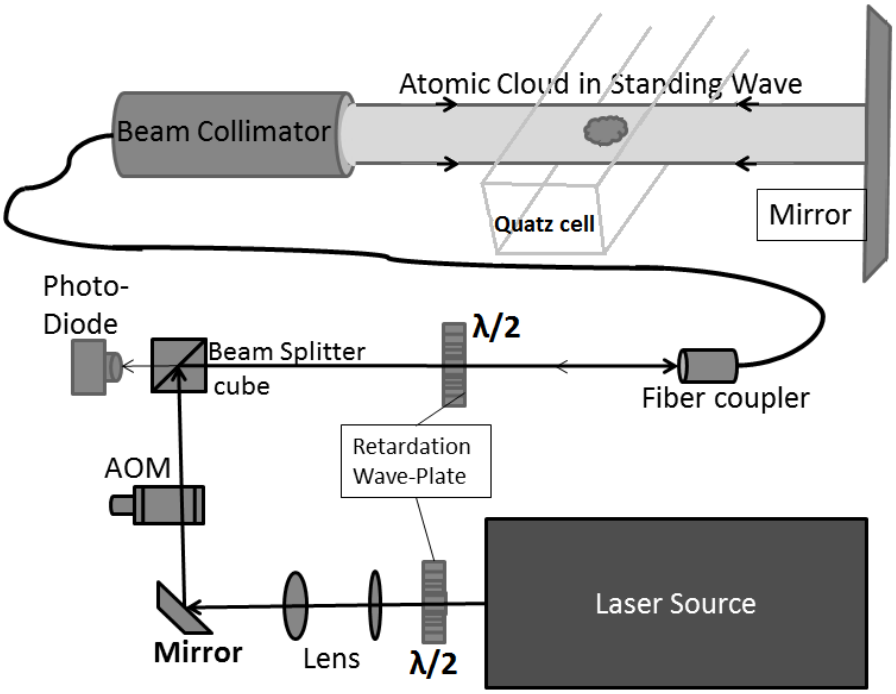

Figure 3.5: schematic of optical lattice setup

controller only. The observed frequency drift of the laser was < 50 MHz/Hr. At detuning of order few GHz, this drift is negligible.

3.3 Coils and Magnetic Field

Rb atoms, being magnetically active in the ground states, lend additional features that can be controlled by magnetic field. Trapping of atoms in MOT, Zeeman slower for fast loading, pumping to a certain magnetic sublevel, trapping in light-free potential; magnetic trap, etc. are few of such examples. For each of these stages the required magnetic field has different spatial profile and the strength. In some cases, the field is varied with time to produce time averaged effect on the potential. In most of the cases, control over field is needed which can only be done by using coils to produced field. Permanent magnets are also used for certain parts where the field is set fixed, but tunability becomes more difficult. It is easy for controlling small field, but when the question comes for controlling high fields the task becomes more challenging. The following subsections contain details about the different fields that are needed for different stages.

3.3.1 Quadrupole Coil

A pair of coils in so called anti-Helmholtz configuration creates field which is quadrupole in space. The field at the center of symmetry is zero. The magnitude increases linearly as we go away from the center (see fig. 3.6). The same coil is used for MOT as well as the magnetic trap, current through the magnetic trap needs to be high enough to produce desired field gradient. Therefore it should be able to carry high enough current, we used 18 SWH enameled copper wire for making the pair of coils. We wound the coil on a delerin made bobbin which has a cap to cover the entire coil inside. This is needed for supplying water flow through the coils to keep it cool. Each of the coils was made with 8 layers and each layer contains 22 turns. The field gradient with the pair, was found to be nearly 8 Gauss/cm·A. Calculations show that the required field gradient for the magnetic trap is about 250 Gauss/cm. Therefore, around 30 Amp. of current is needed. The resistance of the coil was measured to be about 0.9 Ω. Therefore the power dissipated through the coil will be about $I^2R = 30^2 \times 0.9 = 810$ W at maximum field. To dissipate this much of power, continuously water flow through the bobbin is very effective. To make it even more effective, we keep the temperature of the flowing water about 16^0C.

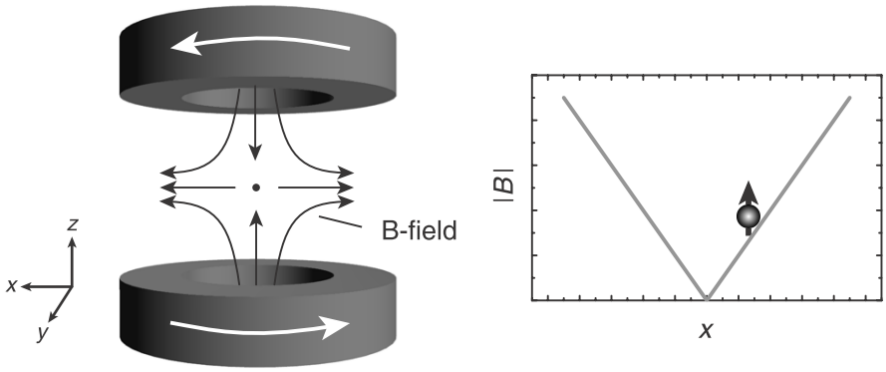

Figure 3.6: schematic of optical lattice setup

3.3.2 Shimming Coils

Since the quartz cell is surrounded by many different instruments that produce magnetic field which can be harmful for while performing some experiments with the atoms. Magnetic field due to earth can also cause trouble. Stray magnetic field can affect while pumping which is done before transferring atoms to magnetic trap. Also, while imaging atoms get split into

different sublevels and only some of the atoms might absorb the imaging beam. To nullify the field three Helmholtz pairs of coils in orthogonal direction, surrounding the quartz cell is placed. The current in each pair is set by optimizing the signal on the atoms. One of the best ways to find the right current is by optimizing the number of atoms in optical molasses. Generally the current in the coils are less than 1 A for compensating the stray field.

3.3.3 Zeeman Slower

As discussed in the previous chapter, Zeeman slower works on the idea of keeping the atoms always in resonance with the laser coming from the opposite direction to ensure continuous force. Assuming constant force and hence constant deceleration, the velocity of atoms at the different positions inside the Zeeman slower follow parabolic profile (see fig. 4.1). The desired field profile for fixed laser detuning was obtained by setting up a condition on the field for which the force throughout the length remains constant. This is done by compensating the Doppler shift by Zeeman shift. The beam of atoms coming from the oven follows Maxwell-Boltzmann distribution. To capture atoms with velocity higher than the average velocity, which ensures that majority of the atoms should get slowed down; laser beam is far detuned from the main transition line. We use the detuning from the transition $\mathbf{F = 2 \rightarrow F' = 3}$ line by about 80 MHz. For this detuning, the atoms with starting velocity about 250 m/s get slowed down to velocity about 25m/s which is good enough for loading in MOT. As it can be seen in the fig 4.1, the direction of field is opposite at the right side, this is important to make sure that the Zeeman slower beam should not interact with the atoms in MOT. This can be understood by following argument: Since the atoms remain in resonance throughout the length of Zeeman slower, therefore, the slowed atoms when they exit the slower should be at resonance at a field about -70 Gauss. Due to the high field the detuning of the laser is kept higher and atoms near the center of MOT do not come in resonance.
The theoretical field profile, the simulated profile and the measured profile matches well. The velocity of the atoms at different position is also plotted on the same plot.

The desired field profile is generated by initially simulating a coil with varying number of turns in each layer using programming in Matlab. To generate field with two different signs, two different such coils, carrying different current, are used. Following is the detail of number of turns in each layer for

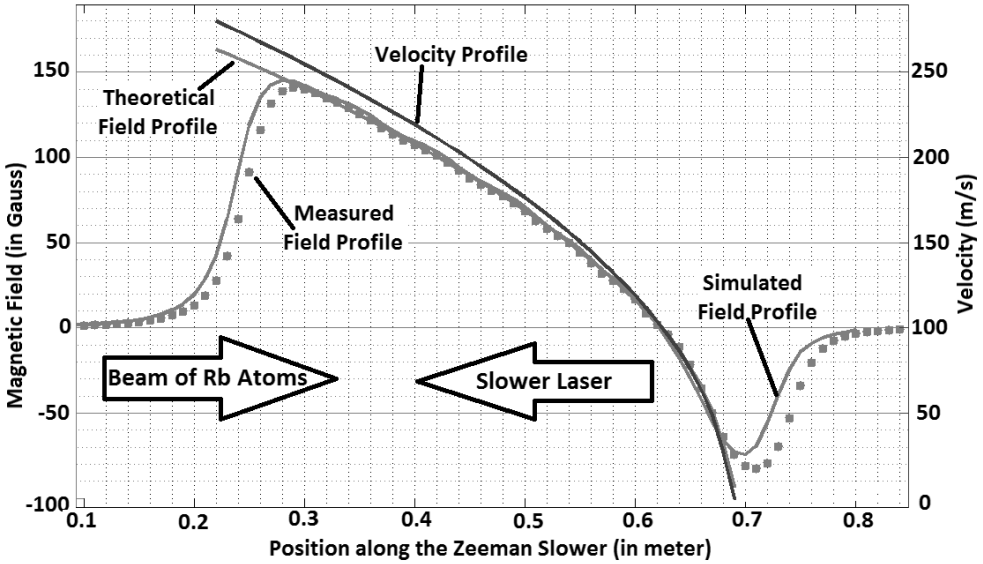

Figure 3.7: Various filed profile and velocity profile of the Zeeman slower

the two coils:

$$positive\ coil \quad = \quad 94\ 81\ 67\ 50\ 31\ 15\ 7\ 2 \tag{3.6}$$

$$negative\ coil \quad = \quad 20\ 15\ 4\ 10 \tag{3.7}$$

The coils were wound on a 80 cm long steel tube with outer diameter 38 mm (see fig 3.8). Current in the positive coil is 8.1 A and in the negative coil is 9A. We used silicone rubber insulated wire for making the coil. It can withstand temperature over 200 ^{o}C; therefore a continuous operation at higher current is possible. The outer diameter of the wire is 3.8 mm.

3.3.4 Current Controller

Fast current control during transfer of atoms from MOT to magnetic trap, after optical pumping, is very important. This is because the longer it takes to increase the field, bigger the size ofl the cloud acquire and the atoms at the outer side see higher field which leads to increase in average energy. As a consequence, the temperature of the cloud increases. Similarly while turning of the field, if the field goes slowly atoms will get enough time to follow the dynamics and they will not remain in the same configuration as they were in the trap. As a result, we might end up imaging little distorted cloud. Additionally, prior to transferring atoms in magnetic trap the cloud size should be as small as possible for the reason mentioned in the beginning of this section.

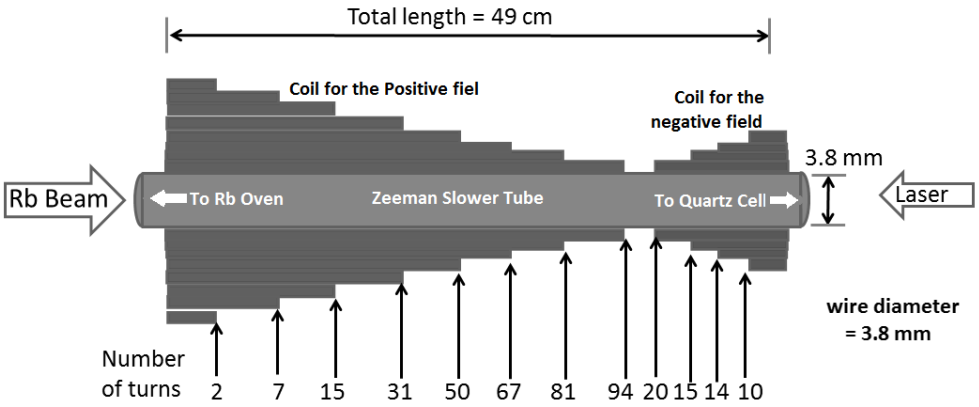

Figure 3.8: Schematic of Zeeman slower turn distribution for different layers

Compression of the cloud is made by increasing the current, in addition to changing certain other parameters, in the MOT coil after atoms get loaded in the MOT. After this step, atoms need to be pumped to a certain magnetic sublevel for which the quadrupole coil needs to be turned off quickly. Also, in the magnetic trap atoms are held for few 10's of second and during that interval the current should be stable as any noise in the current can lead to heating and loss of atoms.

A need for stable and rapid current controller is very important. It becomes challenging task when large inductor and high current needs to be regulated rapidly. We have built a current controller which is a feedback regulated controller. 8 Mosfets in parallel are used to drive current through the coils. Directly connecting the gates makes the current oscillate with very high frequency. This happens due to mismatch in gate threshold voltage and because of that the induced voltage at the gates starts driving the other mosfets randomly. Direct coupling is avoided by placing an R-C circuit between the gates. To reduce the on resistance and to distribute the power dissipation we have used 8 mosfets mounted on a hollow copper heat sink through which cold water flows. A current sensor, is used which gives feedback to the current regulator circuit. Current is controlled by controlling the voltage at the V_{ctrl} terminal. It subtracts from the voltage corresponding to the current sensed by the sensor such that the voltage at the inverting end of the Op-Amp is always zero. To make this condition fulfill, the current through the coil changes accordingly. The inductance of the MOT coil is about 6 mH which gives about 4 ms time to rise the current up to 30 ampere. We have used a switch by additional mosfets to turn off the current

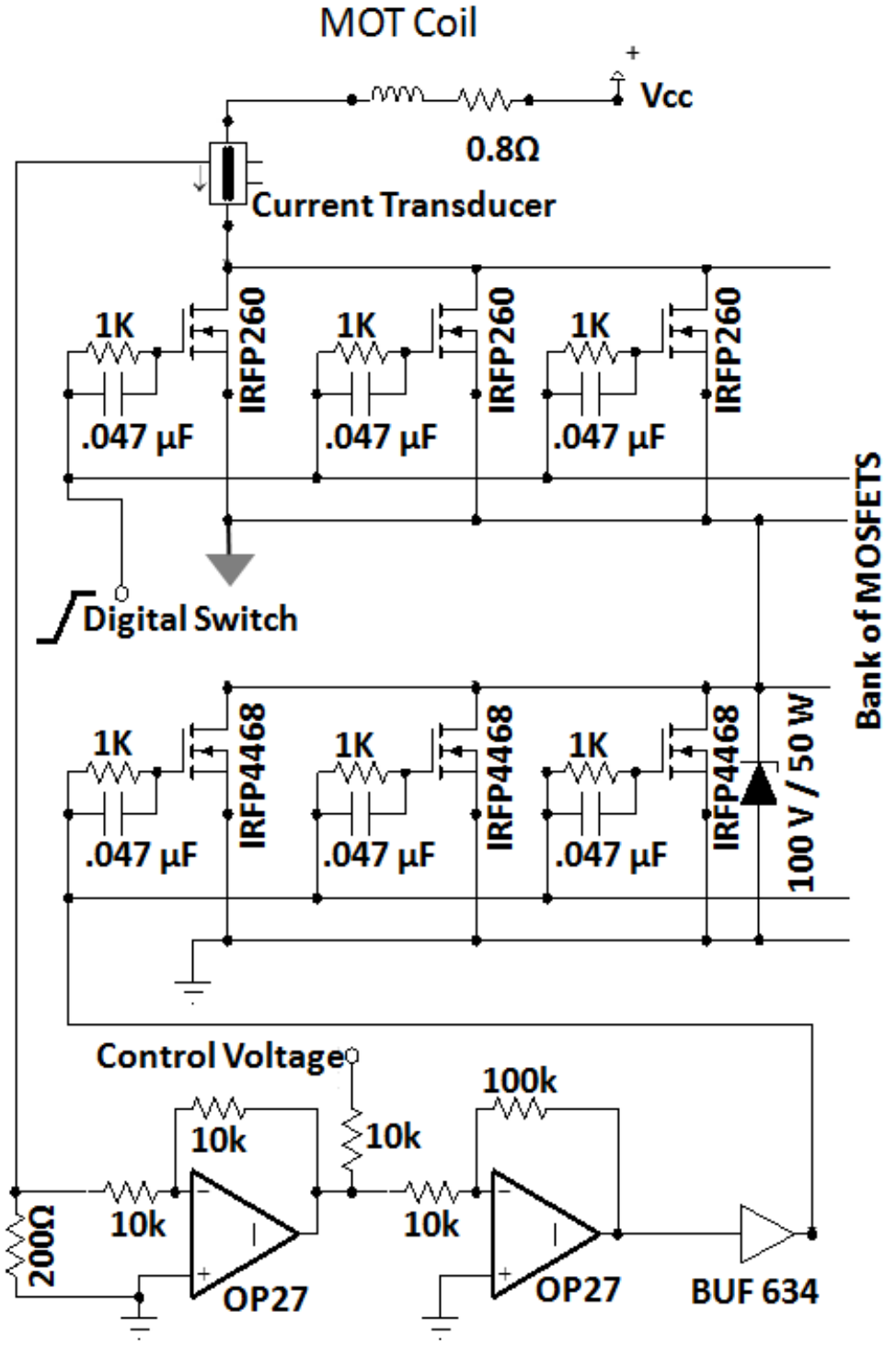

Figure 3.9: circuit diagram of current controller

rapidly and the fall-time we get is less than 600μs. A protection circuit is needed to avoid over-voltage across the mosfets, because while switching off the current rapidly, the voltage induced across the mosfet goes very high for a moment and this is enough to blow the mosfet. We have used a Zener diode of voltage half the threshold voltage of the mosfet. IRFP220 has 200 V_{ds} and the Zener we have used is of 100 V. Additionally, we have measured the noise level in at different constant current, and it is less than 0.3% of the maximum current.
Prior to this, we have tried driving the quadrupole coils with Agilent Power supply (model 6671) by external current control mode. But the rise time and the fall time were not matching the needs of the experiment. The rise time and fall time were more than 20 ms.

3.4 Control and Automation

Many of the steps need precise control over the time when they are active. Control over various other parameters which are decided by a stable voltage is also of very high importance. This includes the amplitude and frequency of light which is controlled by applying appropriate stable voltage to an AOM, control voltage for driving the current through the quadrupole coil, many of the shutters which needs to closed or set open at different steps, synchronized control over the trigger for the imaging beams and the camera. These controls are made possible by using computer programmed sequences which communicates with the hardware in a precise manner.
We use FPGA based DAC card (DIO 64-ViewPoint System) for this purpose. It has 64 number of digital input/output and 16 number of analog input/output controls. The best accuracy on time it gives is less than 50 μs. Labview based user interface is being used to communicate with the hardwares. Although the card is very fast but for certain faster operation, even these cards do not work. Generating kicking potential at a time-scale of few 100's of ns is very important for the kicked rotor experiment. To generate such short pulses with precise control are very difficult with the card. We have used a function generator AFG 100 to generate such short pulses. The time when such pulses need to be generated is controlled by a trigger pule from the card and the function generator gives a burst of those pulses.

Chapter 4

Results

Experiments performed with cold atoms reveal many fundamental phenomena which are, in general, very difficult with systems at normal temperatures. Many extreme techniques are involved for preparing the stage for experiments with ultra-cold atoms. The mechanism of cooling and trapping atoms in MOT is the first step towards this direction. We are able to trap more than 10^8 atoms in 20 second with temperature slightly more than $100\mu K$.
For fast loading of atoms in MOT we have used Zeeman slower. The effect of Zeeman slower is clearly seen on the loading rate. The loading rate in MOT increases rapidly when the Zeeman slower is switched-on. This is because trapping of slower atoms is much easier. The effect of Zeeman slower is shown in the fig 4.1. The laser beam making an angle 25^o to the normal of the atomic beam direction is shone and the fluorescence signal is observed on a photo-multiplier tube (PMT). The spectrum is observed by oscillating the laser frequency in a linear fashion. The x-axis is in time which is converted to frequency by comparing the peaks of the saturation absorption of Rb. Once the scale is converted, the shifts $\Delta 1$ and $\Delta 2$ are calculated. Using following formulae we get the velocity of the atoms.

$$\Delta = kvsin\theta \tag{4.1}$$

where, k is wave vector of laser beam, θ is the angle which is 25^o. From the calculations, we get the speed of the slowed atoms about 25 m/s and the unslowed atoms about 300m/s. Once the atoms are trapped in MOT, they are compressed for further experiments, by increasing field gradient. This step is very sensitive towards alignment of the magnetic field and the six beams crossing. MOT can form even when the beams crossing points are not exactly matching with the quadrupole field center. In that case while compression, the cloud position can shift. This is because of the increasing dominance of field gradient for trapping atoms. This situation leads to oscillatory variation

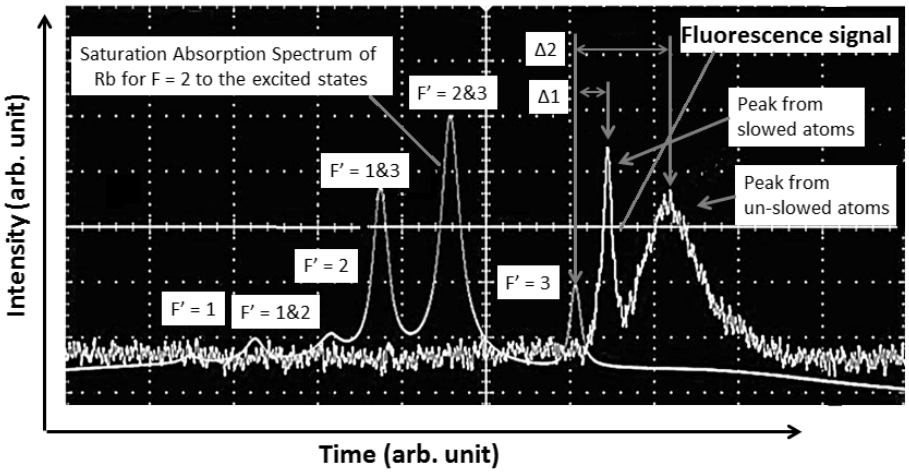

Figure 4.1: Effect of Zeeman slower on the beam of atoms. The fluorescence signal from the atoms shows the peaks of slowed and un-slowed atoms.

of size of the cloud even after switching off the trapping fields which is known as 'breathing mode' (see fig. 4.2). This is signal of bad alignment of the beams with the field. For smaller holding time in the 'compressed MOT' stage the oscillation frequency is higher. Both the frequency and the amplitude decreases as the holding time is increased to 20 ms. It can be understood this way: The atoms do not get enough time to thermalize after the compression, and hence the free expansion does not exactly follow Maxwell-Boltzmann statistics. Whereas if enough time is given, the atoms get thermalized hence they behave as a thermal cloud. After the compression of atoms they are further cooled by polarization gradient cooling. In the attached figure 4.3 the temperature of atoms as a function of laser detuning and polarization gradient cooling time is shown. Though the temperature is very high ($\sim 200\mu$ K), but this plot shows the time and detuning dependence of temperature. The temperature goes down as detuning is increased as well as the time of cooling. The temperature is high because the previous steps were not optimized which we got corrected later. And the temperature we got after polarization gradient cooling below 20 μK which was sufficiently low enough to perform the experiments with delta kicked rotor.

In the experimental realization of kicked rotor, the main quantity of interest that we observe is the average energy growth as a function of number of kicks. We measure temperature because it is a good estimate for the average energy. It can be seen in the graph (see fig. 4.4), the temperature

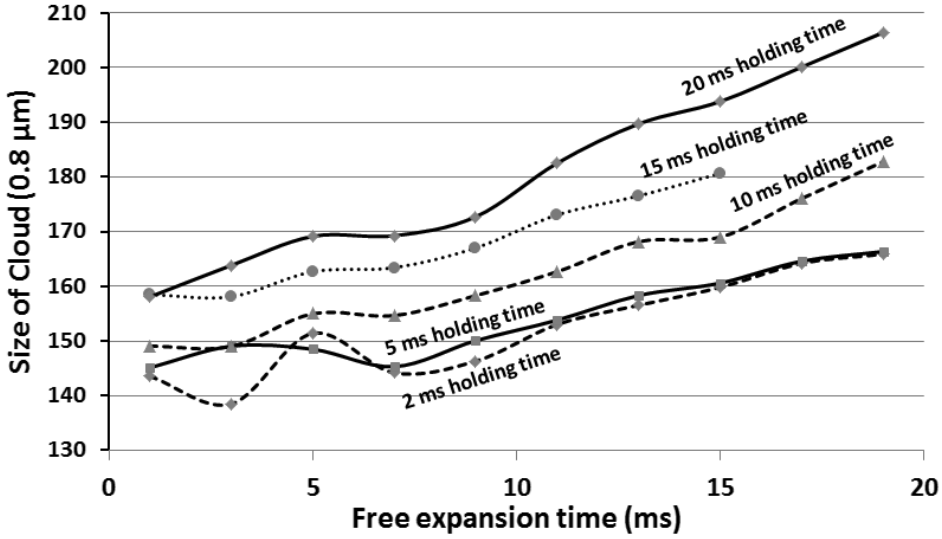

Figure 4.2: The size of the cloud oscillates during free expansion

saturates after initial linear growth, which is a symbol of a delta kicked rotor in quantum regime[15]. The temperature is measured by taking two different time-of-flight images. We sum the rows of the image to get a 1 dimensional peaked curve which is approximately a gaussian-like. The standard deviation of the curves for two different time-of-flight is used to calculate the temperature. We have taken images after 12 ms and 20 ms when the cloud was released. Longer free expansion time helps mapping the momentum distribution very precisely. Since the atoms after getting kicks evolve as per the momentum distribution they acquire. For longer time the position of each atom is decided by the momentum of the atom and hence their spatial distribution is a map of initial momentum distribution. Imaging after longer than 20 ms with our system is limited by the size of the camera chip because the expansion of the cloud covers the whole sensor.
For certain technical issues the data for classical delta rotor was not taken immediately. After resolving the problem we took new set of data and working on measuring the momentum distribution which is even better way to understand the dynamics of the particles in kicked system. The straight line is extrapolated from the data-points of the initial few ($\leq$12) kicks.

The saturation curve is as per the experiments performed earlier by various other groups [18, 16, 17]. We loaded 5×10^6 atoms in MOT, which was further compressed and cooled down to 20μK. The size of the cloud was used to be less than 300 μm. The beam width of the optical lattices is about 1 mm and hence the size of the cloud is much smaller than this. This is

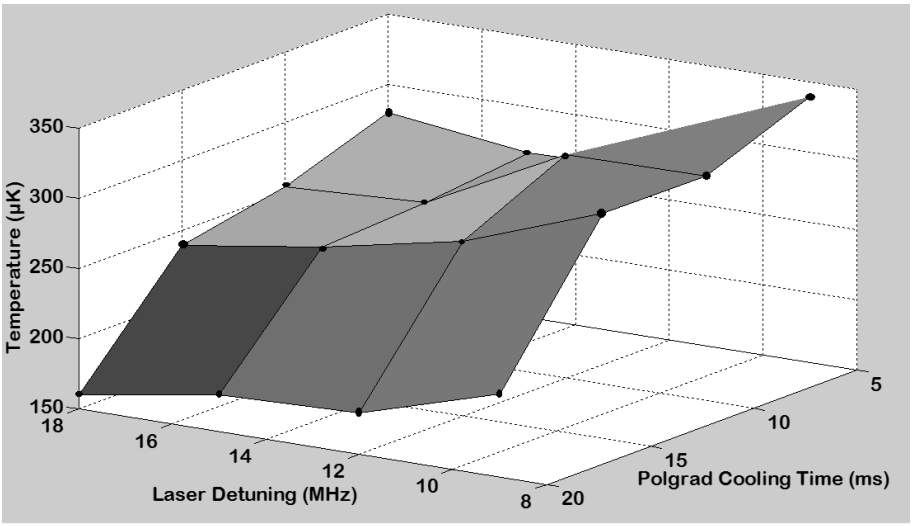

Figure 4.3: Detuning and cooling time dependence of the temperature in the polarization gradient cooling stage

one of the reasons why cloud size should be small. While kicking period, the cloud size increases in addition to it falls under gravity. The combined effects should not let the cloud go outside the lattice beam. The standing wave generated by the laser beam was shone to atoms with pulse time 400 ns and periodicity 50μs. We have given a maximum of up to 100 number of kicks. The total time for free-fall is 5ms, hence the distance the cloud falls is $1/2 \times g \times t^2 = 125\mu$m. Since this length is smaller than the beam width, the atoms do not fall out the beam.
Another set of experiment for realization of kicked rotor is done by giving certain fixed number of kicks and varying time-period between the kicks.

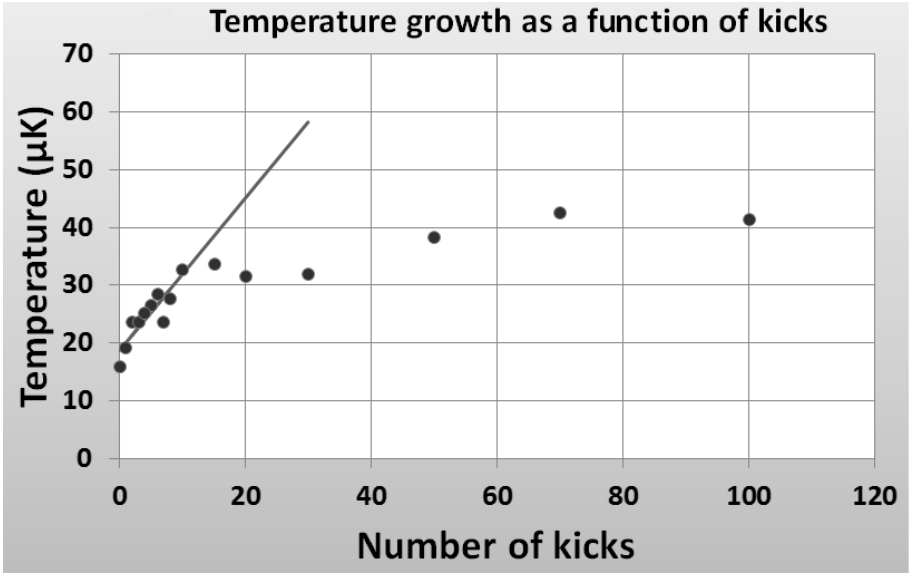

Figure 4.4: Saturation in temperature growth as a function of number of kicks can be seen; the result of dynamical localization.

Chapter 5

Discussions

In this chapter, we discuss the various features of a kicked rotor problem. A kicked system can be used for a possible alternative of creating optical lattices for realization of many-body problem. A brief description about the future plan to realize the Lévy delta kicked rotor is also mentioned.

5.1 Discussions

Despite the simplicity of the problem, a delta kicked rotor shows a variety of interesting results[16, 17, 19]. One of the interesting results is in the area of chaos which leads to localization in the dynamics of the quantum kicked rotor. This result gives us a tool to observe the situation where the transition from quantum to classical dynamics occurs. There is no clear understanding on this particular case as of now[19]. Properties of atoms, electrons and other microscopic systems have experimentally been verified with satisfactory results predicted by quantum mechanics. On other hand, macroscopic objects exactly follow the rules of classical mechanics. At some point both the limits should merge to explain certain phenomena at the boundary. It would be interesting to explore the boundary to 'see' how the transition occurs.
One of the explanations of the transition from quantum world to classical world is the phenomena of decoherence. When a system is in quantum domain, it shows the various phenomena such as interference, collapse of state, superposition of state etc. Of these, interference is one the most important features which leads to the different behavior a quantum system. The key concept behind interference is the associated phase with each state which has no classical analog. An isolated system in coherent state always respects the phase term and, therefore, it sustains the quantum nature. The situation

changes drastically as the environment is allowed to interact with the system, and as a consequence, the phase of each particle do not remain preserved. This is the situation when the phenomena of interference begin to diminish. The outcome is now governed by the classical mechanics. The event of loss of phase relation is also known as decoherence.
Decoherence, in a system, can be induced by many mechanisms. Few of them are spontaneous emission, collisions, randomness and noise, etc. Experiments have been performed [17, 16] with delta kicked rotor to show the effect of these mechanisms to induce decoherence in a system. On-resonance light was used to introduce scattering rate induced decoherence by Amman et al [16]. In an other experiment, by Klappauf et al[17], the effect of dissipation and loss has been observed. All these experiments also rely on the exponential dependence of the decoherence rate. The experiment that we target to perform, Lévy quantum kicked rotor, in our lab shows more interesting features. In presence of specially created noise – the waiting time distribution – the de-coherence does not follow exponential form. This is very interesting, since the way decoherence time depends upon the many parameters (disscussed in chapter 1) does not hold true in this particular case.
Current technologies aim at simulating many complex systems such as many-body problems using quantum mechanical emulator. Quantum computation is another technique in development. The basic need for these studies is preparation of a pure quantum state with extended decoherence time. Ultra-cold atoms provide the initial condition, but the de-coherence time is decided by the interaction with the environment. With our experiment, we will be able to study the circumstances when the decoherence time gets extended.
Additionally, a periodic kicked system shows many parallels with a pure crystal. The Floquet states, which are analogous to Bloch states, are observed. The dynamical localization, which is equivalent to Anderson localization in a crystal with impurities, shows another such similarity. The Floquet states are general form of solution to a periodic time dependent problems. The time between kicks, τ shows exactly the same effect as the spatial periodicity of a crystal does. Certain modifications can be made to realize various properties of a many-body system. Instead of giving just one kick, two kicks can be shone closely separated in time after a period to create a situation which is equivalent to lattice with basis. In general, many such kicks can be given in burst after a period. This will create lattice with many bases.
Probing many-body system using this analogous arrangement would give some advantages and disadvantages. Among the main advantages, creation of precise control over the periodicity, wide range of periodicity, creating a noise either in potential or in periodicity would be the few such examples. Varying the periodicity would be much easier than that in the optical lat-

tices. Creating lattice with basis would be more difficult with the optical lattices. It needs to be worked out theoretically and implemented experimentally to see the practicality of this model. The possible disadvantages could be while switching the potential, especially when the field needed for certain interaction happens to be very high. Another disadvantage is when the time required for certain minimum number of kicks happens to be larger enough such that the cloud gets expanded way beyond the potential region. It is not very clear if this model can be used to create analogy for a three dimensional crystal.

5.2 Future Plan

With the current achievement of atoms at temperature below 20 μ K, our next goal is to give kicks which are not periodic but they are chosen from a suitable waiting time distribution. For, this we need to generate such numbers and feed it to an arbitrary function generator which controls the AOM for the optical lattice beam. We have seen in the simple delta kicked rotor experiment, the saturation in energy starts showing up only after about 15 kicks. Because the number is too low, this would make it difficult to conclude that the outcome for Lévy kicked rotor is due to the statistics. The idea to make the conclusion reliable is based on using different set of such periodicity distributions. This can be done by picking up randomly a set of periodicity from a pool of waiting time distribution data sets. This requires multiple repetition of the experiment with same fixed parameters.
The sequence for the experiments would start from loading about 5×10^6 atoms in MOT. The further compression and cooling would be performed to make the size smaller than 300μm at temperature below 20μK. As the atoms are released from the trap, they will be pumped to a given ground state, **F** =2. After that the kicking pulses should be turned in the presence of weak repump beam to make sure that the atoms should not occupy the other ground state. After the kicks are given, the cloud would be allowed to expand freely for few ms ($\sim$ 20ms). Pulses of imaging beam would be shone to take the image. Images for different expansion times would further be processed to extract out the information of momentum distribution. Our interest is to show the average energy growth which should match with the result predicted in chapter 2 (see fig 2.8)

References

[1] T. W. Hänsch and A. Schawlow, "Cooling of gases by laser radiation," *Optics Communications*, vol. 13, no. 1, pp. 68 – 69, 1975.

[2] D. Wineland and H. Hehmelt, "Proposed $10^{-14}\delta\nu/\nu$ laser fluorescence spectroscopy on TI^{+} mono-ion oscillator," *Bull. Am. Phys. Soc.*, vol. 20, no. 637, 1975.

[3] S. Chu, J. E. Bjorkholm, A. Ashkin, and A. Cable, "Experimental observation of optically trapped atoms," *Physical Review Letters*, vol. 57, no. 3, p. 314, 1986.

[4] E. L. Raab, M. Prentiss, A. Cable, S. Chu, and D. E. Pritchard, "Trapping of Neutral Sodium Atoms with Radiation Pressure," *Physical Review Letters*, vol. 59, no. 23, pp. 2631–2634, 1987.

[5] A. Einstein *Nature*, vol. 3, no. 6877, 1925.

[6] S. N. Bose, "Plancks Gesetz und Lichtquantenhypothese," *Zeitschrift Für Physik*, vol. 26, no. 1, pp. 178–181, 1924.

[7] E. Cornell, M. Anderson, J. Ensher, D. Jin, M. Matthews, and C. Wieman, "Bose-Einstein condensation in an ultracold gas," 1996.

[8] W. Ketterle and N. J. Van Druten, "Bose-Einstein condensation of a finite number of particles trapped in one or three dimensions," *Physical Review A*, vol. 54, no. 1, pp. 656–660, 1996.

[9] S. Chu, "Cold atoms and quantum control.," *Nature*, vol. 416, no. 6877, pp. 206–210, 2002.

[10] I. Bloch, "Ultracold quantum gases in optical lattices," *Nature Physics*, vol. 1, no. 1, pp. 23–30, 2005.

[11] I. Bloch, J. Dalibard, and W. Zwerger, "Many-Body Physics with Ultracold Gases," *Reviews of Modern Physics*, vol. 80, no. 3, pp. 885–964, 2007.

[12] L. Essen and J. V. L. Parry, "An Atomic Standard of Frequency and Time Interval: A Cæsium Resonator," *nat*, vol. 176, pp. 280–282, Aug. 1955.

[13] W. Markowitz, R. G. Hall, L. Essen, and J. V. L. Parry, "Frequency of cesium in terms of ephemeris time," *Phys. Rev. Lett.*, vol. 1, pp. 105–107, Aug 1958.

[14] T. Udem, R. Holzwarth, and T. W. Hänsch, "Optical frequency metrology," *nat*, vol. 416, pp. 233–237, Mar. 2002.

[15] G. Casati, B. V. Chirikov, F. M. Izraelev, and J. Ford, "Stochastic behavior of a quantum pendulum under a periodic perturbation," *Stochastic Behavior in Classical and Quantum Hamiltonian Systems*, vol. 93, no. 5, p. 334, 1979.

[16] H. Ammann, R. Gray, I. Shvarchuck, and N. Christensen, "Quantum Delta-Kicked Rotor: Experimental Observation of Decoherence," *Physical Review Letters*, vol. 80, no. 19, p. 4111, 1998.

[17] B. Klappauf, W. Oskay, D. Steck, and M. Raizen, "Observation of Noise and Dissipation Effects on Dynamical Localization," *Physical Review Letters*, vol. 81, pp. 1203–1206, Aug. 1998.

[18] F. L. Moore, J. C. Robinson, C. Bharucha, P. E. Williams, and M. G. Raizen, "Observation of Dynamical Localization in Atomic Momentum Transfer: A New Testing Ground for Quantum Chaos," *Physical Review Letters*, vol. 73, no. 22, pp. 2974–2977, 1994.

[19] H. Schomerus and E. Lutz, "Nonexponential decoherence and momentum subdiffusion in a quantum Levy kicked rotator.," *Physical Review Letters*, vol. 98, no. 26, p. 260401, 2007.

[20] P. van der Metcalf, Harold J., Straten, *Laser Cooling and Trapping*. Springer, 2002.

[21] J. Dalibard and C. Cohen-Tannoudji, "Laser cooling below the Doppler limit by polarization gradients: simple theoretical models," *Journal of the Optical Society of America B*, vol. 6, no. 11, p. 2023, 1989.

[22] H.-J. Stöckmann, *Quantum Chaos an Introduction.* Campbridge University Press.

[23] P. W. Anderson, "Absence of Diffusion in Certain Random Lattices," *Phys. Rev.*, vol. 109, pp. 1492–1505, Mar. 1958.

[24] S. Bize, Y. Sortais, M. Santos, C. Mandache, A. Clairon, and C. Salomman, "High-accuracy measurement of the rb-87 ground-state hyperfine splitting in an atomic fountan," *Europhys. Lett.*, vol. 45, no. 558, 1999.

[25] G. P. Barwood, P. Gill, and Q. Rowley, "Frequency measurements on optically narrowed rb-stabilised laser diodes at 780 nm and 795 nm," *Appl. Phys. B*, vol. 53, no. 142, 1991.